AD-A185 545 SMOKE HAZARDS RESULTING FROM THE BURNING OF SHIPBOARD PAINTS PART 3(U) GEORGIA INST OF TECH ATLANTA F W WILLIAMS ET AL. 18 SEP 87 NRL-9043 N00014-78-C-0432 1/1

UNCLASSIFIED F/G 11/3 NL

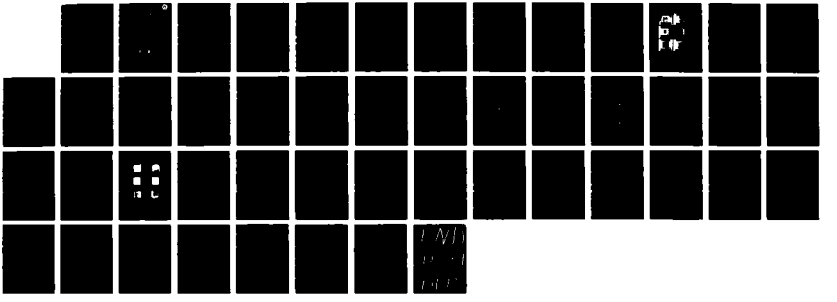

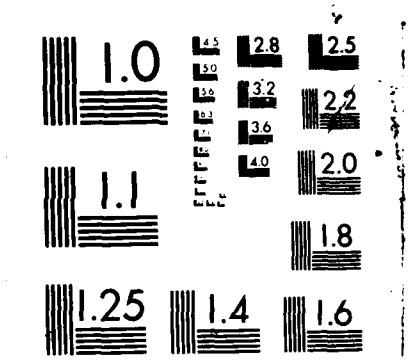

Naval Research Laboratory
Washington, DC 20375-5000

NRL Report 9043

Smoke Hazards Resulting From the Burning of Shipboard Paints—Part III

F. W. WILLIAMS

Fire/Personnel Safety Research and Technology Center
Chemistry Division

E. A. POWELL AND B. T. ZINN

Georgia Institute of Technology
Atlanta, Georgia

September 18, 1987

A185 545

SECURITY CLASSIFICATION OF THIS PAGE

REPORT DOCUMENTATION PAGE

1a REPORT SECURITY CLASSIFICATION UNCLASSIFIED	1b RESTRICTIVE MARKINGS
2a SECURITY CLASSIFICATION AUTHORITY	3 DISTRIBUTION / AVAILABILITY OF REPORT Approved for public release; distribution unlimited.
2b DECLASSIFICATION / DOWNGRADING SCHEDULE	
4 PERFORMING ORGANIZATION REPORT NUMBER(S) NRL Report 9043	5 MONITORING ORGANIZATION REPORT NUMBER(S)
6a NAME OF PERFORMING ORGANIZATION Naval Research Laboratory 6b OFFICE SYMBOL (*If applicable*) Code 6183	7a NAME OF MONITORING ORGANIZATION Naval Sea Systems Command
6c ADDRESS (*City, State, and ZIP Code*) Washington, DC 20375-5000	7b ADDRESS (*City, State, and ZIP Code*)
8a NAME OF FUNDING / SPONSORING ORGANIZATION Naval Sea Systems Command 8b OFFICE SYMBOL (*If applicable*) Code 05R	9 PROCUREMENT INSTRUMENT IDENTIFICATION NUMBER ONR Contract N00014-78-C-0432
8c ADDRESS (*City, State, and ZIP Code*) Washington, DC 20362-5101	10 SOURCE OF FUNDING NUMBERS PROGRAM ELEMENT NO: 63514N; PROJECT NO: S0364SL; TASK NO: ; WORK UNIT ACCESSION NO: DN880-171

11 TITLE (*Include Security Classification*)
Smoke Hazards Resulting From the Burning of Shipboard Paints—Part III

12 PERSONAL AUTHOR(S)
Williams, F. W., Powell, E. A.,* and Zinn, B. T.*

13a TYPE OF REPORT	13b TIME COVERED	14 DATE OF REPORT (*Year, Month, Day*)	15 PAGE COUNT
Interim	FROM 9/81 TO	1987 September 18	48

16 SUPPLEMENTARY NOTATION
*Georgia Institute of Technology, Atlanta, Georgia 30032

17 COSATI CODES			18 SUBJECT TERMS (*Continue on reverse if necessary and identify by block number*)	
FIELD	GROUP	SUB-GROUP	Smoke	Light scattering
			Combustion products	Polymeric materials
			Particle size analysis	Fire hazards

19 ABSTRACT (*Continue on reverse if necessary and identify by block number*)

Investigations have been continued to evaluate the hazards caused by smoke formation in shipboard fires. The physical properties of the smoke particulates generated during combustion were determined for two types of paints used by the U.S. Navy in ships and submarines. These were a chlorinated alkyd paint and an intumescent paint. The physical properties measured were particle size distribution, mean particle diameter, mass fraction of fuel converted to particulates, optical density, particle refractive index, and particulate volume fraction. The dependence of these properties on the temperature of the test-chamber atmosphere (room temperature to a maximum of 300°C) and the mode of combustion (flaming or smoldering) was determined for both materials.

The results of this study indicated that both paints produce smoke with a log-normal particle size distribution during smoldering combustion in the room temperature tests. Optical measurements made during these

(Continues)

20 DISTRIBUTION / AVAILABILITY OF ABSTRACT	21 ABSTRACT SECURITY CLASSIFICATION	
☒ UNCLASSIFIED/UNLIMITED ☐ SAME AS RPT ☐ DTIC USERS	UNCLASSIFIED	
22a NAME OF RESPONSIBLE INDIVIDUAL Frederick W. Williams	22b TELEPHONE (*Include Area Code*) (202) 767-2476	22c OFFICE SYMBOL Code 6180

DD FORM 1473, 84 MAR 83 APR edition may be used until exhausted
All other editions are obsolete

SECURITY CLASSIFICATION OF THIS PAGE

GPO U.S. Government Printing Office 1985-607-647

19. ABSTRACT (Continued)

tests show that both paints produce smoke particulates with mean diameters that vary with time between 0.6 and 1.2 μm. Under these conditions the chlorinated alkyd paint produces pale yellow spherical liquid droplets, while the intumescent paint produces a mixture of light tan and white solid particles. For flaming combustion of the chlorinated alkyd paint, irregularly shaped aggregates of small soot particles with a mean aggregate diameter of about 1.2 μm are produced. Flaming combustion of the intumescent paint is weak and intermittent, occurring only in tests conducted in air heated to 100°C or above. Mean particle diameter increases slightly during flaming combustion of the chlorinated alkyd paint as the temperature of the chamber atmosphere is increased. Increasing the ventilation air temperature greatly reduces the total amount of smoke produced during nonflaming combustion of the intumescent paint as well as the resulting light obscuration. Under room temperature and nonflaming conditions, the light obscuration (optical density) obtained with the intumescent paint is much greater than that produced by burning an equal mass of chlorinated alkyd paint under the same conditions.

CONTENTS

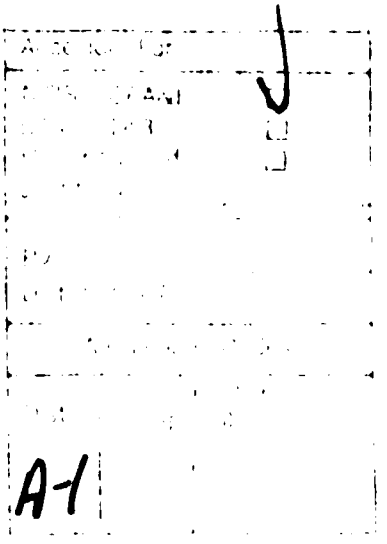

SMOKE HAZARDS RESULTING FROM THE BURNING OF SHIPBOARD PAINTS—PART III

INTRODUCTION

This report describes the efforts conducted under the broad heading "The Determination of the Smoke Hazards Resulting from the Burning of Shipboard Materials Utilized by the U .S. Navy." This work was performed during the period September 1, 1981 through August 31, 1983. Specifically, it is a continuation of work done during the previous three years to determine the physical and chemical properties of smoke particulates generated during the combustion of representatives of three classes of materials abundantly present on Navy ships. In the present investigation, smoke was physically characterized for interior fire retardant paints. Two types of paint were investigated: a chlorinated alkyd paint (as specified by DOD-E-24607) and an intumescent paint (Ocean 9788). The aims of this investigation were to identify the conditions under which large quantities of smoke would result in severe light obscuration.

EXPERIMENTAL FACILITIES

The smoke research program described here has been conducted by using the following facilities that have been developed at the School of Aerospace Engineering, Georgia Institute of Technology: (a) a combustion products test chamber, (b) a combustion products sampling system, and (c) an in situ optical aerosol measurement system.

The ventilated combustion products test chamber (CPTC) is described in detail in Refs. 1 through 5 and is capable of simulating a wide variety of environmental conditions that may be encountered in actual fire situations. Specifically, the design of the CPTC permits easy control and measurement of the following variables during the combustion of small samples of materials:

- the mode of combustion (i.e., flaming vs smoldering combustion),
- the sample radiant heating rate (up to 10 W/cm^2),
- the sample weight loss during the test,
- the composition of the ventilating gas surrounding the sample,
- the temperature of the ventilation gas (up to 650°C), and
- the option to test the sample under either vertical or horizontal mounting.

The CPTC's aerosol sampling system elucidates particle size distributions and the total particulate mass generated.

Manuscript approved December 31, 1986

In addition to the data obtained by sampling techniques, an in situ optical aerosol measurement system is used to make simultaneous mean particle size and concentration measurements. With this optical smoke analysis system, measurement of scattered blue-green laser light (λ = 0.488 μm) at forward angles of 5° and 15° provides time-resolved data describing the average size of the smoke particles. Measurement of transmitted red (λ = 0.633 μm) and blue-green laser lights provides the optical densities of the smoke at these two wavelengths. For nonabsorbing particles (usually produced by nonflaming combustion) the transmitted light measurements along with the mean particle size measurements also yield the refractive index and volume fraction of the smoke particles. For absorbing particles (i.e., soot), measurements of 90° scattered blue-green light intensities parallel to and perpendicular to the plane of polarization of the incident light beam provide the additional data necessary to determine the complex refractive index of the smoke particles. Details of the optical system are available in Refs. 6 and 7.

An on-line data acquisition system using a Hewlett-Packard 2100 minicomputer is being used for acquiring, reducing, and plotting all of the optical data with the exception of the 90° scattering data, which must be reduced using the Control Data Corporation (CDC) Cyber 730 computer at Georgia Tech's computer center.

TEST PROCEDURES AND CONDITIONS FOR SMOKE PHYSICAL PROPERTIES MEASUREMENTS

The first material to be tested, a chlorinated alkyd paint, was provided by the Navy. The second material, Ocean 9788 intumescent paint, was supplied by the manufacturer, Ocean Chemicals. The tests were performed by using the CPTC, the aerosol sampling system and the in situ aerosol measurement system.

For tests conducted in room temperature ventilation gas, the physical analysis of the smoke particulates determined the following smoke properties: (a) the particle size distribution, (b) the mass fraction of fuel converted to particulates, (c) the evolution of the mean particle diameter with time, (d) the light obscuration by the particles (i.e., optical density), (e) the particle refractive index, and (f) the volume fraction (i.e., volume concentration) of the particles. For the tests conducted in hot ventilation gas, items (a) and (b) above were not determined since the aerosol sampling system can not be operated at high temperatures. The sample mass loss as a function of time was also determined for most of the tests.

The dependence of the above quantities on the following experimental conditions was determined: the temperature of the test chamber atmosphere and the mode of combustion (i.e., flaming or smoldering combustion). Table 1 shows the test matrix to which the two paints were subjected. All of the tests were conducted in the horizontal sample orientation, and in all of the tests the sample was exposed to a radiant heat flux of 5 W/cm^2. The particulate size distributions using cascade impactor sampling were determined for all room temperature tests. In the flaming tests, the pyrolysis products generated by exposure of the sample to the 5 W/cm^2 radiant flux were ignited by a small propane pilot flame. Finally, in all tests of the chlorinated alkyd paint the CPTC ventilation gas consisted of air flowing at a volumetric rate (before heating) of 425 l/min, while in all tests of the Ocean 9788 intumescent paint a lower flow rate of 142 l/min was used. Because of the decrease in density of the ventilation air during heating, the volumetric flow rate of the heated air during the high temperature tests was higher as shown in Table 1. Additional tests at 150 and 200°C were also conducted for reasons to be discussed later. The flow rates for these additional tests are also given in Table 1 (Tests 7 and 8).

Table 1 — Test Matrix for Interior Fire Retardant Paints

	Radiant Flux W/cm^2	Ventilation Gas Temperature (°C)	Mode of Combustion	Ventilation Gas Composition	Flow Rate of Heated Ventilation Gas (l/min)	
					Chlorinated Alkyd	Intumescent
1	5.0	25	Nonflaming	Air	425	142
2	5.0	100	Nonflaming	Air	532	178
3	5.0	300	Nonflaming	Air	817	273
4	5.0	25	Flaming	Air	425	142
5	5.0	100	Flaming	Air	532	178
6	5.0	300	Flaming	Air	817	273
7	5.0	150	Nonflaming	Air	–	202
8	5.0	200	Nonflaming	Air	675	225

The following sections of this report present the smoke particulate physical properties data for the fire retardant paints tested during this research program. Brief discussions of each of the measured parameters are given in Appendix A of Ref. 8.

SMOKE PHYSICAL PROPERTIES DATA FOR CHLORINATED ALKYD PAINT

Description of Material and Sample Preparation

This paint conforms to the military specification (DOD-E-24607) for interior semigloss enamel based on chlorinated alkyd resin [9]. This enamel is formulated to provide a decorative coating or dry film that, although degraded by heat, will not spontaneously ignite in the event of exposure to fire. The color of the paint tested was Soft White, Formula No. 124. Table 2 lists the chemical composition of this paint.

Regardless of color, the paint consists of 57.0% to 60.5% by mass pigments (primarily barium sulfate and titanium dioxide), 20.5% to 23.0% volatiles, and 18.5% to 21.0% nonvolatile vehicle (45% chlorinated dibasic acid). The density of the wet paint ranges from 1.73 to 1.80 kg/l.

Samples of the chlorinated alkyd paint were prepared by brushing it onto 5.1-cm (2-in.) squares of cold rolled steel substrate 0.79 mm (1/32 in.) thick. The average weight of the substrates was 19.0 g, which was just below the limit imposed by the force transducer. The substrates were first cleaned with acetone, then 10 thick coats of paint were applied with a small brush over a 17-day period with 1 to 4 days drying time between coats. The average dry mass of paint applied in this manner was 10.66 g with a standard deviation of 0.49 g. This yields an average dry film thickness of 2.3 mm based on a dry film density of 1.79 g/cm^3. Storage time under ambient laboratory conditions for these samples ranged from 2 to 44 weeks.

Table 2 — Composition of Chlorinated Alkyd Paint

Ingredient	Percent by Mass of Enamel
Barytes[a]	34.90
Titanium dioxide	23.27
Chlorinated alkyd resin[b]	30.91
Paint thinner (petroleum spirits)	9.97
Lead naphthenate	0.39
Cobalt naphthenate	0.16
Antisettling agent	0.33
Antiskinning agent	0.07

[a]Minimum of 98.0% barium sulfate.
[b]Chlorine, in the form of chlorinated dibasic acid, minimum of 4.2% by mass of enamel.

Tests in Room Temperature Ventilation Air

Both flaming and nonflaming tests of the chlorinated alkyd paint have been conducted in room temperature ventilation air (25°C) with a radiant flux of 5 W/cm^2. For all of these tests the ventilation air flow rate was 425 l/min (15 ft^3/min). The results of these tests are presented in Figs. 1 through 5 and in Tables 3 and 4.

Figure 1 presents the curves of sample mass vs time for flaming and nonflaming combustion of the chlorinated alkyd paint samples, and Table 3 gives the peak mass loss rates obtained from these curves. These curves show that significant mass loss caused by pyrolysis begins about 2 mins. after the sample is first exposed to the radiant heat flux. A peak mass loss rate of about 0.4 mg/cm^2-s occurs after about 4 mins. of exposure in the nonflaming mode. During flaming combustion, the peak mass loss rate is about 50% greater and occurs about a minute earlier than for the nonflaming mode. Under both flaming and nonflaming conditions, slightly more than 80% of the initial sample mass remains as char, with slightly less char remaining in the flaming case. This is not surprising, since about 75% of the dry paint consists of nonvolatile inorganic pigments. Figure 2 shows the char residues for both nonflaming and flaming tests. In both cases the residue has a thin, brittle, white surface skin with large cracks revealing black flaky char layers underneath. Some swelling of the char occurs during combustion with a maximum char thickness of about 6 mm. In Fig. 2 it is seen that the residue left after flaming combustion also has more cracks in the surface skin than the residue left after nonflaming combustion, and it also has numerous small blisters in the surface skin along the edge of the largest cracks. It is likely that these blisters are due to the higher local surface temperatures associated with the flaming combustion of pyrolysis gases issuing from these cracks.

Smoke particle size distributions were obtained by using the cascade impactor for both flaming and nonflaming combustion of the chlorinated alkyd paint samples at the radiant flux of 5 W/cm^2. Figure 3 shows these size distributions as cumulative curves generated by plotting the percentage of particulate weight having particle diameters less than a given particle size vs the particle size on log-normal probability coordinates. In both cases, a straight line gives a good fit to the cascade impactor data (plotted points), which indicates that the size distribution is log-normal for both flaming and nonflaming modes. Table 4 gives the mass median diameters D_{MMD} and standard deviations σ_g obtained from these curves. For *nonflaming* combustion the particulates consist of pale yellow spherical liquid

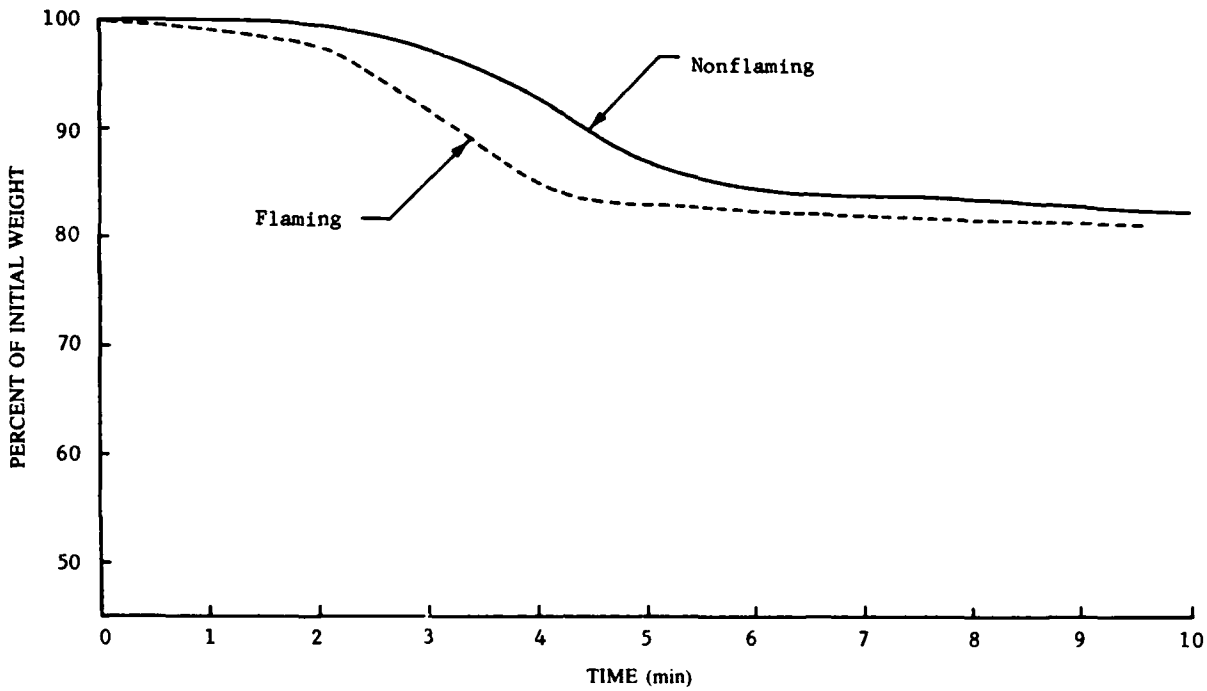

Fig. 1 — Sample weight losses for flaming and nonflaming combustion of chlorinated alkyd paint exposed to a radiant flux of 5 W/cm^2 in room temperature ventilation air (25°C)

Table 3 — Samole Weight Loss Data for Chlorinated Alkyd Paint on Steel Substrate

Mode	Ventilation Air Temperature (°C)	Radiant Flux (W/cm^2)	Peak Mass Loss Rate (mg/cm^2-s)	Char Residue (Percent of Initial Weight)
Nonflaming	25	5.0	0.40	82.1
Nonflaming	100	5.0	0.40	81.2
Flaming	25	5.0	0.58	80.8
Flaming	100	5.0	0.82	79.7
Flaming*	200	5.0	0.57	78.5
Flaming	300	5.0	1.12	77.4
Flaming*	300	5.0	1.40	77.7

*Spontaneous flaming ignition occurred during a "nonflaming" test (i.e., no pilot flame).

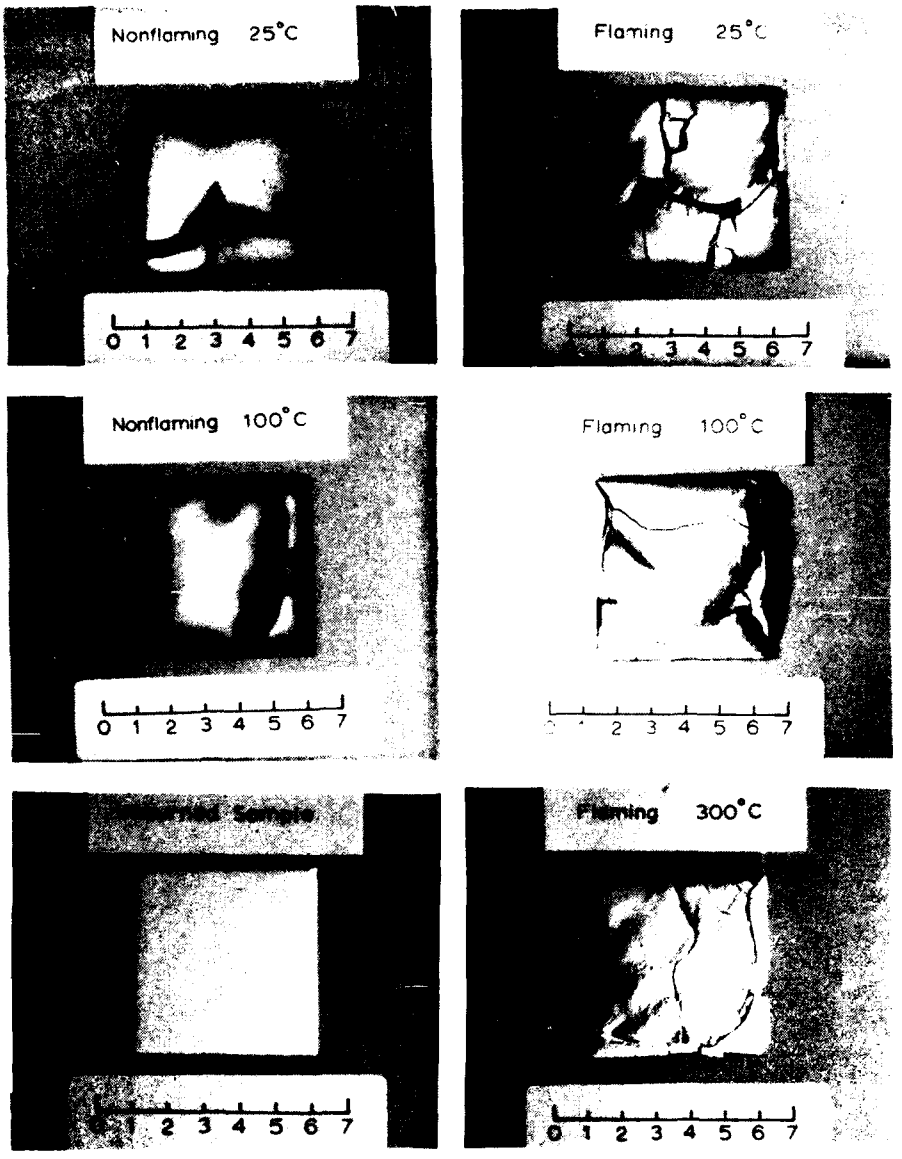

Fig. 2 — Char residues for chlorinated alkyd paint tests
scale is in centimeters

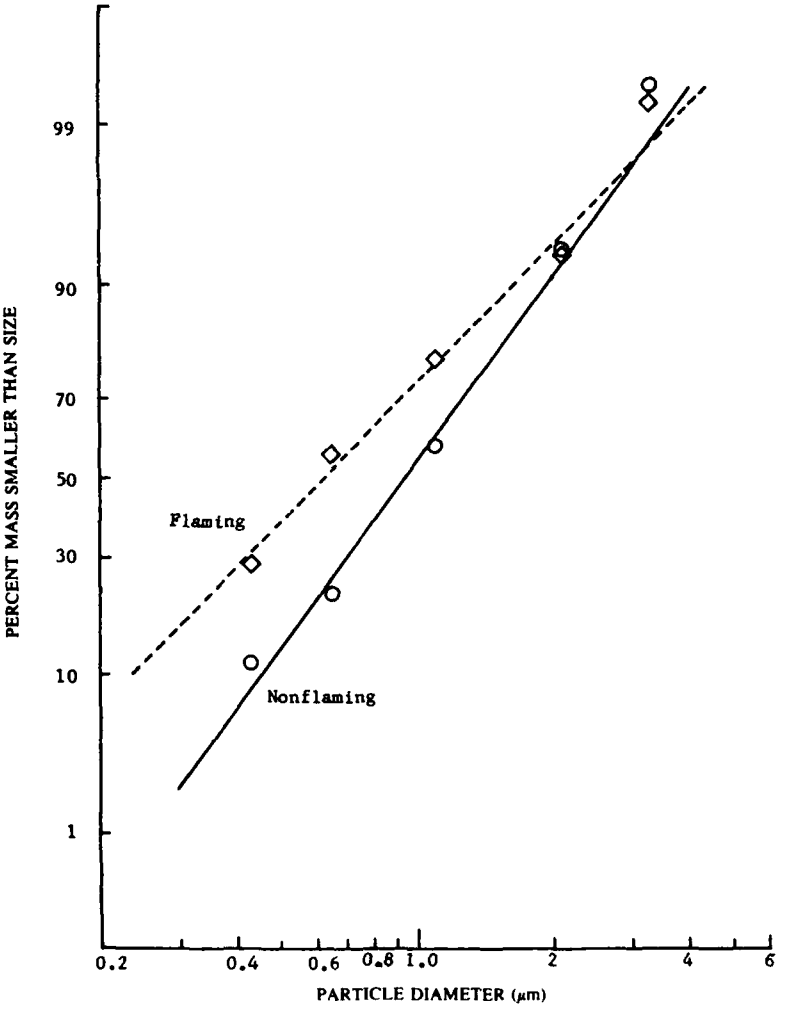

Fig. 3 — Smoke particle size distributions for flaming and nonflaming chlorinated alkyd paint exposed to a radiant flux of 5 W/cm^2 in room temperature ventilation air (25°C)

Table 4 — Smoke Properties Data for Chlorinated Alkyd Paint

Mode	T (°C)	Radiant Flux (W/cm^2)	Γ	D_{MMD} p (μm)	σ_g	OD_{max} (m^{-1})		D_{32}^a (μm)	Time to Peak OD (min)
						Blue	Red		
Nonflaming	25	5.0	0.113	0.94	1.77	0.90	0.79	0.84	4.9
Nonflaming	100	5.0	—	—	—	0.54	0.44	0.82	4.1
Flaming	25	5.0	0.037	0.63	2.16	0.84[b]	0.70[b]	1.17	3.5[b]
Flaming	100	5.0	—	—	—	1.25[c]	1.03[c]	1.20	1.8[c]
Flaming[d]	200	5.0	—	—	—	0.79[b]	0.62[b]	1.21	2.4[b]
Flaming	300	5.0	—	—	—	1.46	1.17	1.29	0.9
Flaming[d]	300	5.0	—	—	—	2.06	1.67	1.26	1.1

[a]Average of data points near OD_{max}.
[b]Second of two peaks.
[c]First of two peaks.
[d]Spontaneous flaming ignition occurred during a "nonflaming" test (i.e., no pilot flame).

droplets with a D_{MMD} of about 0.9 μm. Here the total mass of particulates collected on the cascade impactor was about 13 mg, with about 1.5 mg collected on the last filter (absolute) (<0.43 μm) and the last impactor stage (0.43 to 0.65 μm) and about 4.5 mg on each of the next two impactor stages (0.65 to 1.1 μm and 1.1 to 2.1 μm). Less than 1 mg of these particles were larger than 2.1 μm. For *flaming* combustion, black sooty particulates were collected with a D_{MMD} of about 0.6 μm. The size distribution determination is less accurate than that for the nonflaming mode, because the total mass of particulates collected was only about 4 mg, of which about 1 mg each was collected on the absolute filter (<0.43 μm) and on the last two impactor stages (0.43 to 0.65 μm and 0.65 to 1.1 μm). Smaller amounts were collected (0.6 mg and 0.3 mg) on the next two stages (1.1 to 2.1 μm and 2.1 to 3.3 μm). Traces of soot particles were detected visually on the impactor plates for sizes greater than 3.3 μm, but the quantities collected were too small to detect by weighing (<0.02 mg per stage). These results indicate the particle size distribution obtained for flaming combustion of the chlorinated alkyd paint is considerably broader than that obtained for nonflaming combustion, even though the value of D_{MMD} is smaller in the flaming case.

Sampling data was also used to determine the fraction of the sample mass loss converted to particulates (Γ) for the room temperature tests. Table 4 gives the values of Γ that show that for nonflaming combustion under 5 W/cm^2 radiant flux about 11% of the total mass loss appears as particulates, while for flaming combustion under similar conditions slightly less than 4% of the mass loss is converted to soot particles.

The in situ optical system was used to obtain mean particle diameters D_{32} and optical densities produced by flaming and nonflaming combustion of the chlorinated alkyd paint samples. Figure 4 gives a comparison of mean particle sizes for flaming and nonflaming combustion, while Fig. 5 gives the corresponding optical densities.

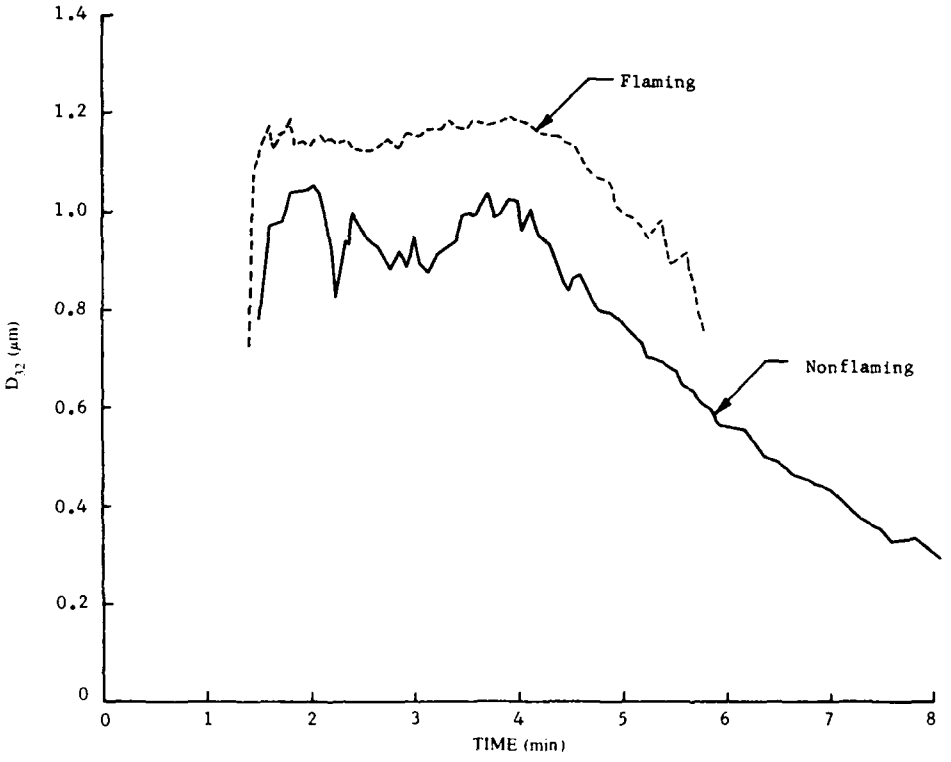

Fig. 4 — Smoke mean particle diameters for flaming and nonflaming combustion of chlorinated alkyd paint exposed to a radiant flux of 5 W/cm^2 in room temperature ventilation air (25°C)

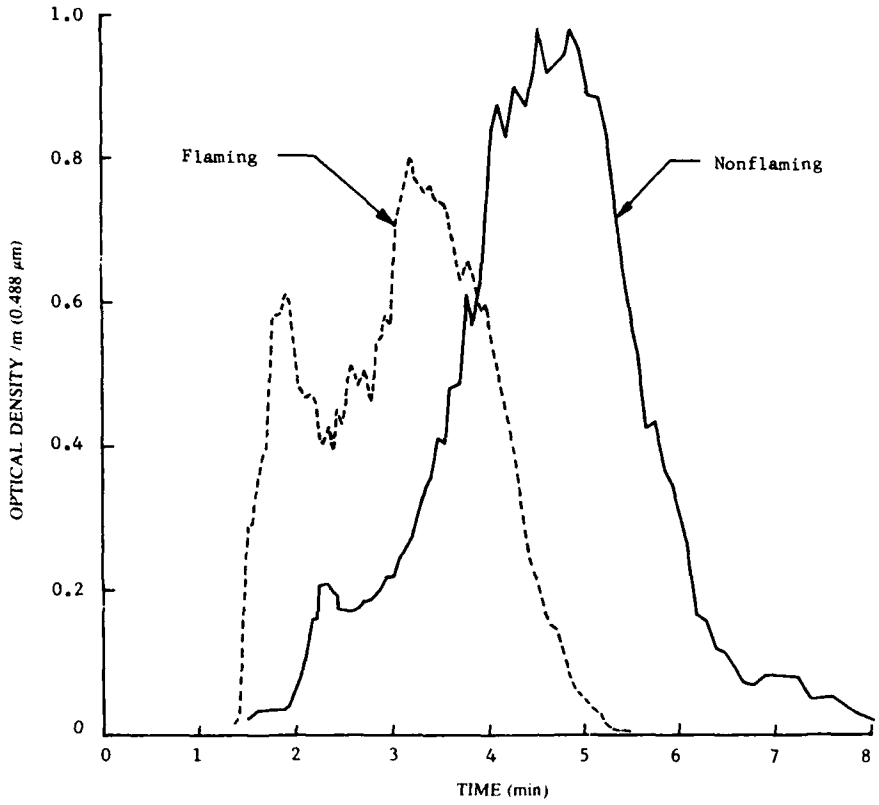

Fig. 5 — Smoke optical densities for flaming and nonflaming combustion of chlorinated alkyd paint exposed to a radiant flux of 5 W/cm^2 in room temperature ventilation air (25°C)

Figure 4 shows that for *nonflaming* combustion in room temperature ventilation air, the mean particle diameters vary between 0.7 and 1.1 μm during the initial stages of pyrolysis and average about 0.85 μm during the time of maximum optical density. This latter value is in very good agreement with the D_{MMD} obtained by cascade impactor sampling (Table 4). During the later stages of pyrolysis the D_{32} decreases gradually to below 0.4 μm as a result of the rapidly declining rate of production of condensible pyrolysis products. For *flaming* combustion, the mean particle diameters are nearly constant throughout the test, ranging between 1.1 and 1.2 μm. The mean diameter obtained optically (D_{32}) is nearly twice that obtained by particle sampling (D_{MMD}) for flaming combustion. This discrepancy is probably due to the nonspherical shape of the soot particle agglomerates produced under flaming combustion.

Figure 5 shows that for *nonflaming* combustion in room temperature ventilation air, the optical density at the blue-green argon line (0.488 μm) rises smoothly to a peak of about 1.0 m^{-1} about 5 mins after initiation of exposure and then smoothly declines. For *flaming* combustion, peak optical density is somewhat lower and occurs earlier in the test. Furthermore, the curves of optical density vs time exhibit two pronounced peaks, the second of these occurring after about 3.5 mins and reaching about 0.85 m^{-1}.

Tests in Heated Ventilation Air

Results of tests of chlorinated alkyd paint samples conducted in hot ventilation air are shown in Figs. 6, 8, and 9 for nonflaming combustion and in Figs. 7, 10, and 11 for flaming combustion. In each figure the room temperature data are also shown for comparison. High temperature data are also given in Tables 3 and 4. In all flaming tests, a small propane pilot flame was maintained throughout the test, and the radiant heat flux was .5 W/cm^2 for all tests. For ventilation air temperatures of 200°C and above, the chlorinated alkyd paint samples ignited spontaneously (i.e., without the pilot flame), therefore nonflaming data was not obtained for the highest ventilation gas temperature.

Figure 6 and Table 3 show that, for *nonflaming* combustion of the chlorinated alkyd paint, heating the ventilation air to 100°C causes pyrolysis to begin earlier but has little or no effect on the peak mass loss rate (0.4 mg/cm^2-s). This moderate increase in ventilation air temperature also results in a slight increase in the total mass of pyrolysis products evolved as reflected in the slight decrease in the amount of char residue. On the other hand, Table 3 and Fig. 7 show that for *flaming* combustion of the chlorinated alkyd paint, increasing the ventilation air temperature results in a significant increase in peak mass loss rate. For flaming tests in 300°C air, the peak mass loss rate (1.1 mg/cm^2-s) was nearly twice that obtained in the room temperature flaming tests. The peak mass loss rate also occurs earlier at elevated ventilation air temperatures. For 300°C ventilation air, half of the mass loss has occurred by 1.3 mins after initiation of exposure, while about 3.2 mins are required for a similar mass loss to occur in the room temperature environment. Heating the ventilation air for the flaming tests also resulted in further small reductions in the percentage of initial mass remaining as char. In each of the flaming tests the pilot flame and radiant heating were maintained for 10 mins. The results of the flaming tests are consistent with increased convective heat transfer to the samples from the hot ventilation gas that results in increased pyrolysis rates and greater amounts of material pyrolyzed.

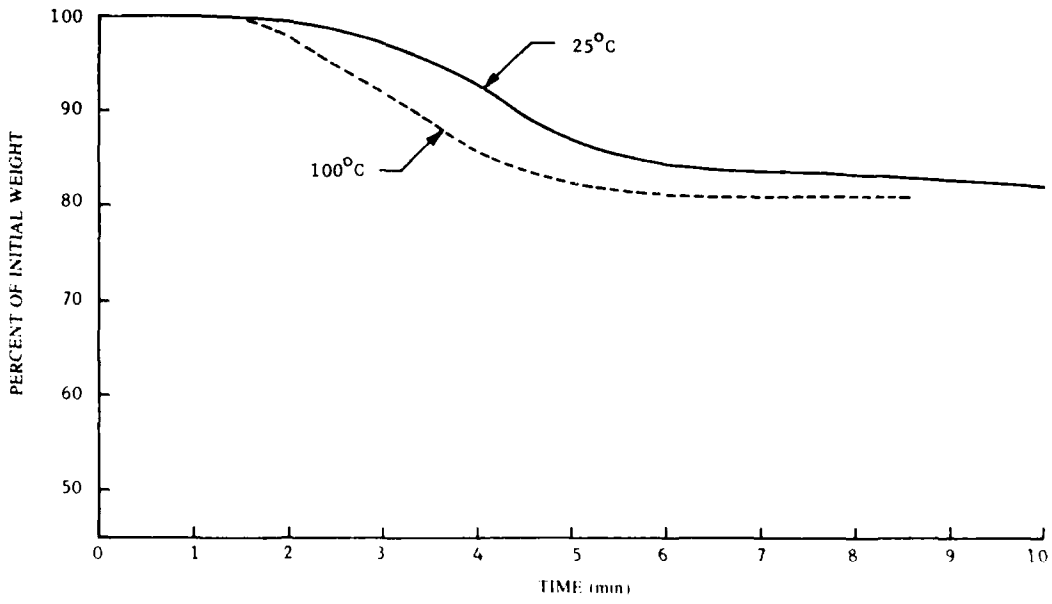

Fig. 6 — Effect of ventilation air temperature on sample weight loss for nonflaming combustion of chlorinated alkyd paint exposed to a radiant flux of 5 W/cm^2

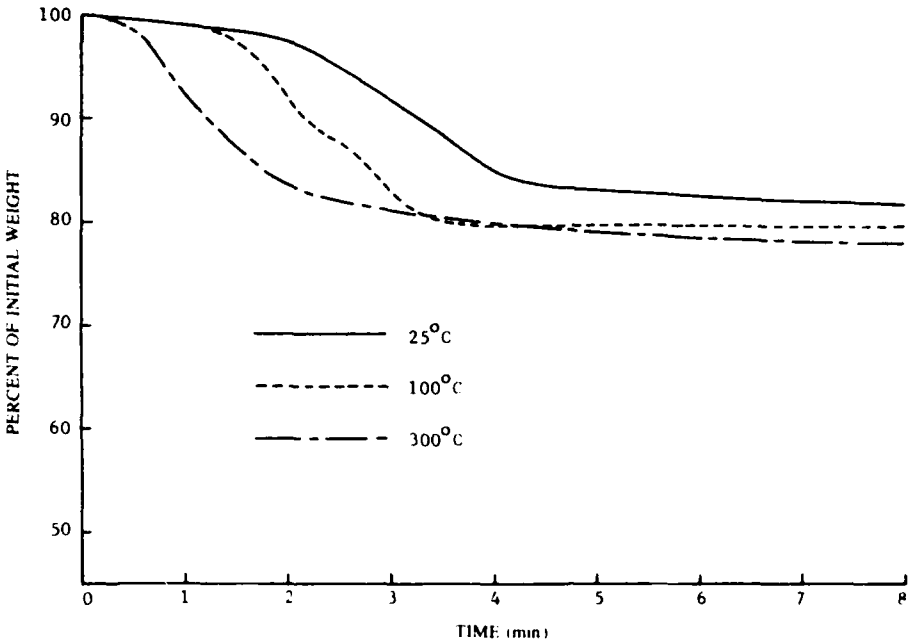

Fig. 7 — Effect of ventilation air temperature on the sample weight loss for flaming combustion of chlorinated alkyd paint exposed to a radiant flux of 5 W/cm^2

Figure 8 presents the comparison of the D_{32}s for *nonflaming* tests of chlorinated alkyd paint conducted in room temperature and 100°C atmospheres. It is seen that this moderate amount of heating has a pronounced effect on the shape of the curve of D_{32} vs time. In contrast to the relatively constant values of D_{32} followed by a gradual decline obtained in room temperature air, at 100°C there is an initial sharp peak in D_{32} of nearly 1.4 μm followed by a short plateau at about 1.0 μm followed by a rapid decline in particle size. In both cases the maximum optical density occurs shortly after the beginning of the final decline in D_{32}. Although the shapes of the curves are different, moderate increases in environmental temperature have little effect on the mean particle diameters obtained near the time of peak optical density (Table 4). It should also be noted that the sharp peak in particle size for the 100°C test occurs at a time when the optical density, and hence the particle volume fraction, is relatively low. Even though pyrolysis begins earlier at 100°C than at room temperature, particulate light scattering is detected later in the higher temperature test owing to the suppressed condensation of the more volatile pyrolysis products.

Figure 9 shows the effect of environmental temperature on optical density (λ = 0.488 μm) for *nonflaming* tests of the chlorinated alkyd paint. The curves in Fig. 9 are based on directly measured values, while the corresponding peak optical densities (λ = 0.488 and 0.633 μm) given in Table 4 have been corrected for the higher ventilation air flow rates caused by the expansion of the ventilation air during the constant pressure heating process. The curves of optical density vs time for the two temperatures are similar in shape, but the peak optical density at 100°C is roughly half that obtained in the room temperature test. The peak optical density also occurs slightly earlier in the hotter ventilation air. These trends are consistent with reduced condensation of pyrolysis products and increased heat transfer to the sample as the ventilation air temperature increases.

Figure 10 shows the effect of ventilation air temperature on the D_{32}s for *flaming* combustion of the chlorinated alkyd paint. For tests in room temperature (25°C), 100°, and 300°C air, the pilot flame was ignited at t = 0, but the ignition of the sample was delayed until sufficient pyrolysis products were evolved to form a combustible mixture. As expected this ignition delay becomes

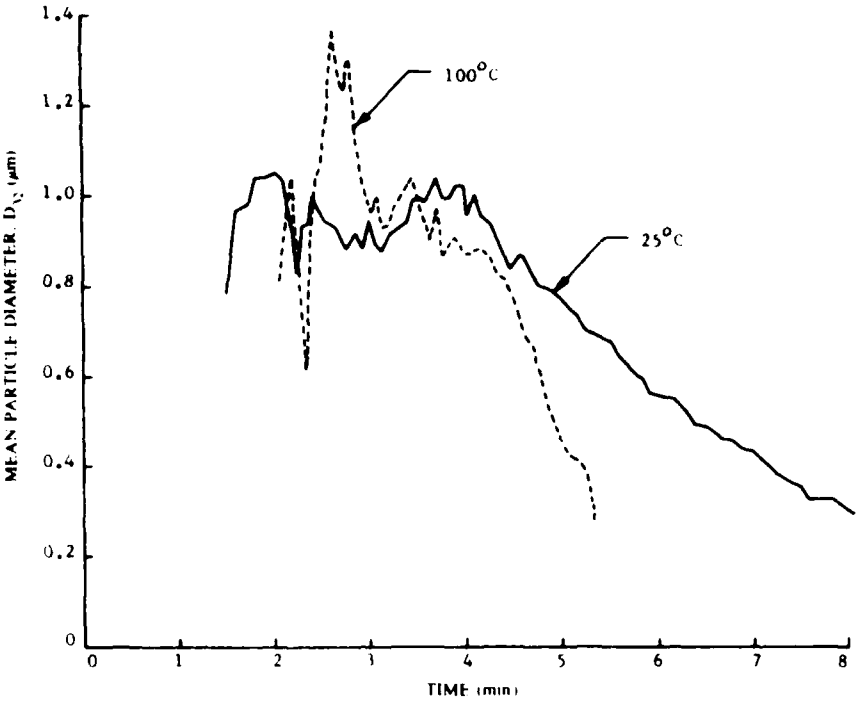

Fig. 8 — Effect of ventilation air temperature on the smoke mean particle diameter for nonflaming combustion of chlorinated alkyd paint exposed to a radiant flux of 5 W/cm²

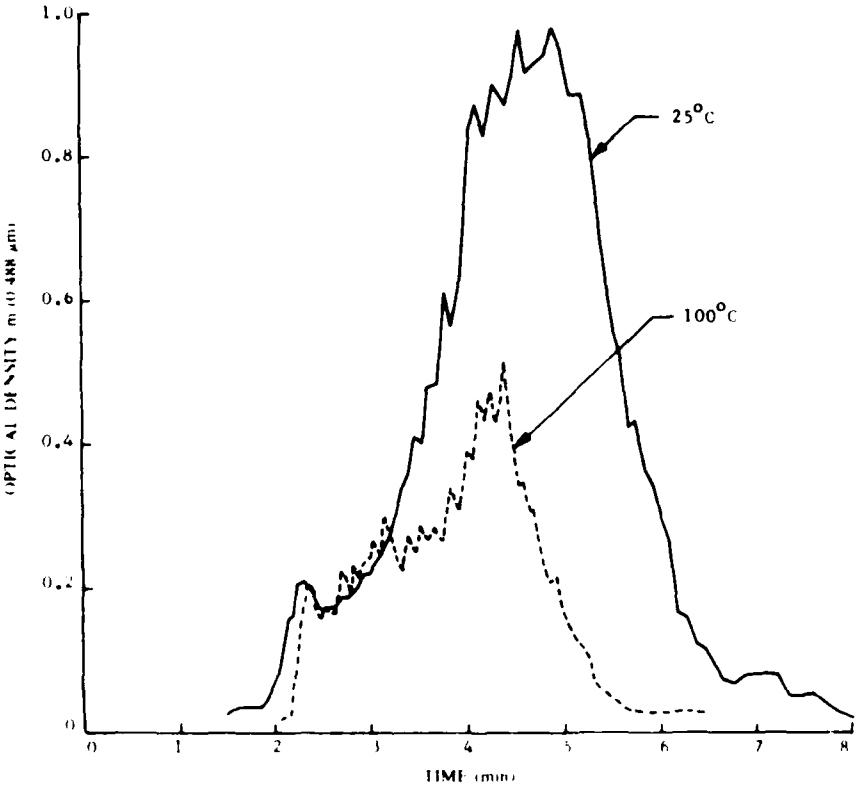

Fig. 9 — Effect of ventilation air temperature on the smoke optical density for nonflaming combustion of chlorinated alkyd paint exposed to a radiant flux of 5 W/cm²

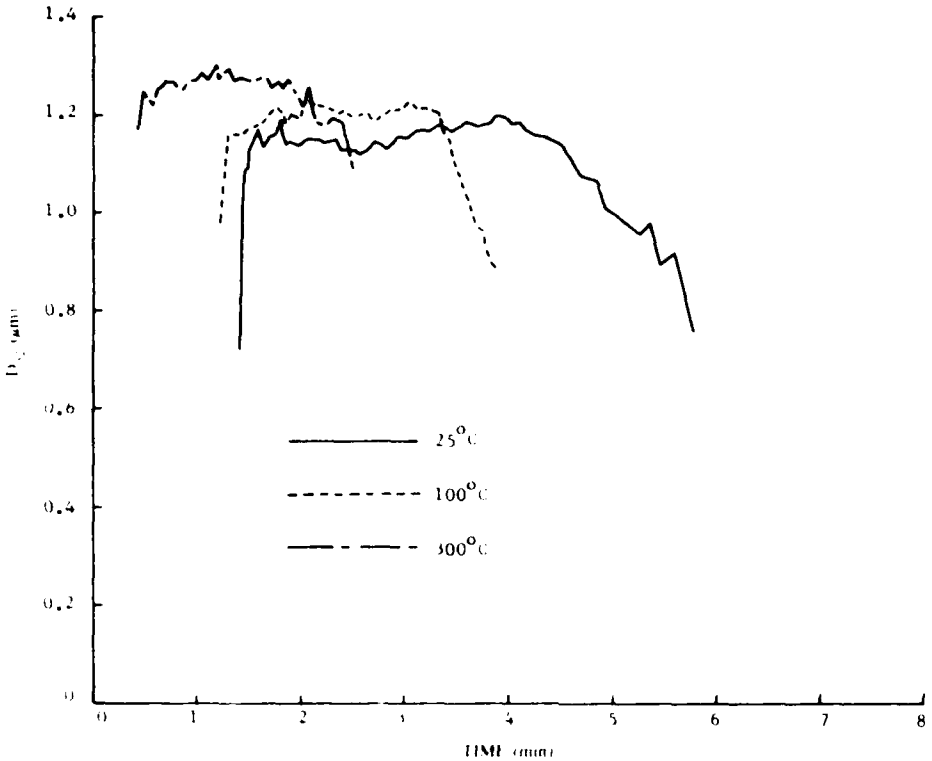

Fig. 10 Effect of the ventilation air temperature on the smoke mean particle diameter for flaming combustion of chlorinated alkyd exposed to a radiant flux of 5 W/cm^2.

shorter as the environmental temperature is increased, as evidenced by the sharp rise in the light scattering and the particle sizes exhibited at the beginning of each curve shown in Fig. 10. These curves and the data in Table 4 also show a small but definite trend of increasing D_{32} as the ventilation air temperature is increased. This behavior has been observed to various degrees for a variety of polymeric materials [3,6,8]. It has been demonstrated experimentally that increasing the temperature of gaseous diffusion flames generally leads to greater quantities of soot and larger soot agglomerates produced within the flame [10]. This is expected to enhance further agglomeration processes in the smoke plume, which accounts for the larger particle sizes observed.

Figure 11 presents the curves of optical density variation with time for flaming combustion of the chlorinated alkyd paint samples at different ventilation air temperatures. The optical density peaks generally occur at earlier times as the environmental temperature increases, and the directly measured peak values of optical density are not significantly influenced by temperature. However, when the dilution effect owing to the increase of the volumetric ventilation flow rate with temperature is taken into account, the peak optical density (λ = 0.488 μm) at 100°C is about 50% higher than at room temperature, while the corresponding increase in peak optical density at 300°C is about 75% (Table 4). For the room temperature and 100°C tests, there were always two prominent optical density peaks with considerable variations in peak heights from one test to another. Thus the OD_{max} values given in Table 4 are averages of the largest peak values over a number of replicate tests. The second peak generally predominated in the room temperature tests, while the first peak was more prominent in the 100°C tests. At 300°C the second peak was either absent or much smaller than the main peak. It thus appears that the two optical density peaks arise from different physicochemical mechanisms, one that is enhanced by increasing temperature (first peak) and one that is suppressed by increasing temperature (second peak).

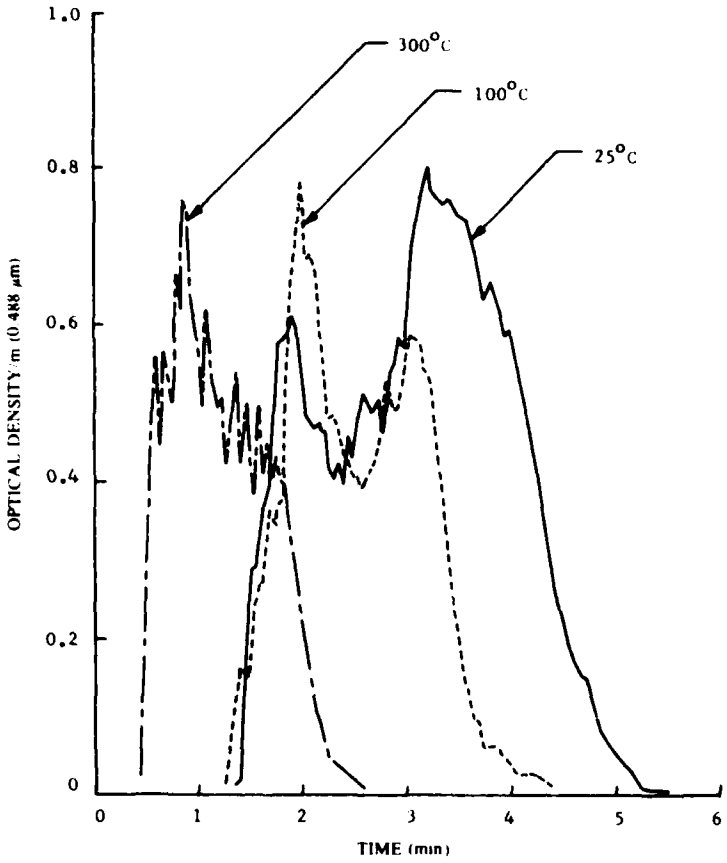

Fig. 11 — Effect of ventilation air temperature on the smoke optical density for flaming combustion of chlorinated alkyd paint exposed to a radiant flux of 5 W/cm^2

Smoke Particle Refractive Index and Volume Fraction

For *nonflaming* tests of the chlorinated alkyd paint, measurement of the ratio of optical densities OD_R/OD_B and the 90° scattering ratio $I_\parallel/I_\perp$ were used to determine the refractive index of the smoke particles. For each test, it was initially assumed that the particles were nonabsorbing ($k = 0$), and the measured values of $I_\parallel/I_\perp$ in blue-green light ($\lambda = 0.488\ \mu m$) along with the previously determined values of D_{32} were used to calculate the corresponding refractive index n_B. Measured OD_R/OD_B values were also used to obtain the refractive index, assuming that $k = 0$ and that n does not vary significantly with wavelength.

Values of n_B determined from the 90° scattering data for a test in room temperature air reveal considerable variations in refractive index with time during a test, as shown by the solid curve in Fig. 12. In this case, the refractive index exhibits a gradual rise from values just below 1.30 to a maximum of nearly 1.375 followed by a gradual decline. Such variations in the refractive index indicate corresponding variations in the chemical composition of the smoke particles (presumed to be mixtures of liquid organic compounds) during the nonflaming test. Near the time of peak optical density, the 90° scattering data gave an average value of n_B of 1.355 (Table 5), while the optical density ratio yielded a smaller value, $n_R = n_B = 1.338$. It is assumed that slightly absorbing particles did not resolve this discrepancy because the Mie theory gives no solution for positive values of k. On the other hand, allowing n to vary with wavelength (with $k = 0$), successfully fitted both sets of data by calculating n_R from the measured OD_R/OD_B values by using the n_B values obtained previously from the $I_\parallel/I_\perp$ data. As shown in Fig. 12 (dashed curve), the refractive index in red light ($\lambda = 0.633\ \mu m$) is slightly smaller than the refractive index in blue-green light ($\lambda = 0.488\ \mu m$) for the middle portion of the test, and it exhibits similar variations with time during this period. The average value of n_R at peak optical density was $n_R = 1.343$.

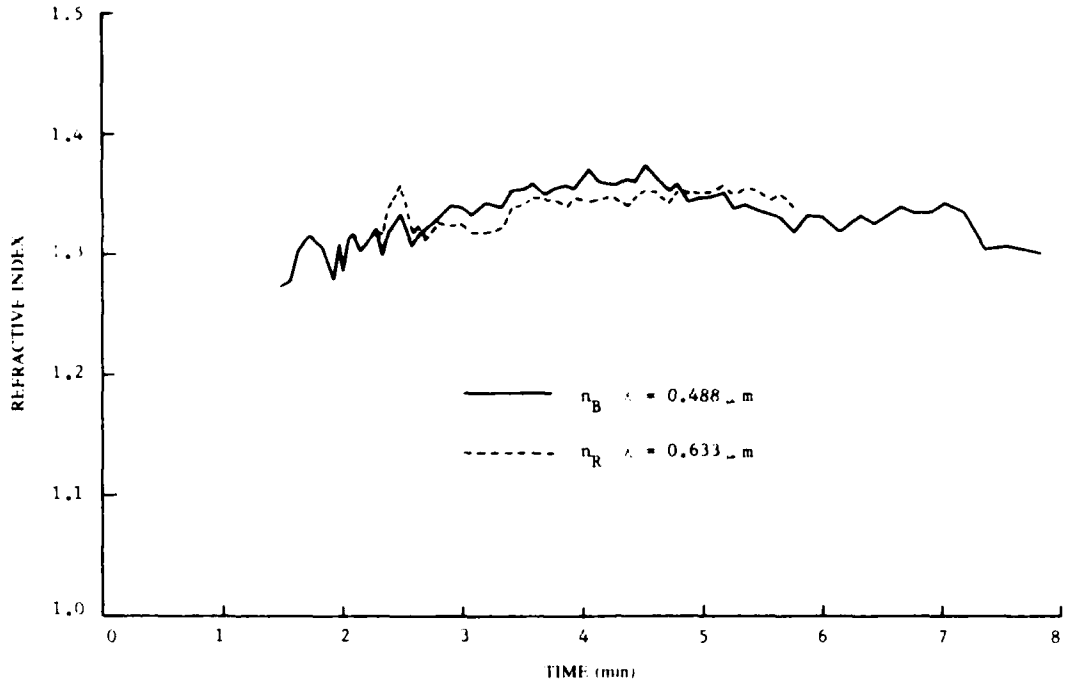

Fig. 12 – Variations of the smoke particle refractive index during the nonflaming combustion of chlorinated alkyd paint exposed to a radiant flux of 5 W/cm^2 in room temperature ventilation air (25°C)

Table 5 — Smoke Refractive Index, Volume Fraction, and Total Volume for Chlorinated Alkyd Paint

Mode	Ventilation Air Temperature (°C)	Radiant Flux (W/cm^2)	Refractive Index m_B (NF) or m_λ (F)	η_λ	Peak Volume Fraction (ppm)	Specific Total Particle Volume (cm^3/g)	Γ/Γ_{25}
Nonflaming	25	5.0	1.355 – 0.0i	—	0.42	0.040	1.00
Nonflaming	100	5.0	1.417 – 0.095i	—	0.26	0.017	0.42
Flaming	25	5.0	1.152 – 0.107i	0.259	0.76	0.054	1.00
Flaming	100	5.0	1.173 – 0.123i	0.294	1.09	0.043	0.76
Flaming[a]	200	5.0	1.154 – 0.109i	0.262	0.79	0.047	0.78
Flaming	300	5.0	1.144 – 0.101i	0.245	1.43	0.050	0.79
Flaming[a]	300	5.0	1.149 – 0.105i	0.254	1.95	0.047	0.75

[a]Spontaneous flaming ignition occurred during a "nonflaming" test (i.e., no pilot flame).

Refractive index values were also measured for smoke particles produced under nonflaming combustion in ventilation air at 100°C. Under the assumption of nonabsorbing particles ($k = 0$) variations in refractive index were again observed as the test proceeded. The refractive index measured during the time of maximum optical density was 1.314 ($\lambda = 0.488\ \mu m$), which was somewhat lower than the corresponding value measured under room temperature conditions (Table 5). The refractive index in red light ($\lambda = 0.633\ \mu m$) was only slightly larger ($n_R = 1.319$) than the values in blue-green light. Both of these values are lower than would be expected for the higher boiling organic compounds that would be expected to condense in the higher temperature atmosphere (Ref. 8, Appendix B).

To investigate the possibility that the particles produced in the 100°C nonflaming tests absorb as well as scatter light (i.e., $k \neq 0$), plots of $I_{\parallel}/I_{\perp}$ and OD_R/OD_B as a function of mean particle diameter D_{32} were constructed. A typical plot for a 100°C test is shown in Fig. 13. By assuming reasonable values of the complex refractive index m_B, good curve fits were obtained by using the Mie theory for various portions of the 90° scattering data. For example, $m_B = 1.422 - 0.10i$ gave a good fit for D_{32} less than 0.85 μm, which includes the data obtained around the time of peak optical density (between 2.5 and 5.5 minutes after start of test). For larger particles ($D_{32} > 0.85\ \mu m$), which were produced during the first 2.5 minutes of the test, $m_B = 1.414 - 0.085i$ gave a better fit. The theoretical curves corresponding to these values of m_B are shown in the upper plot of Fig. 13.

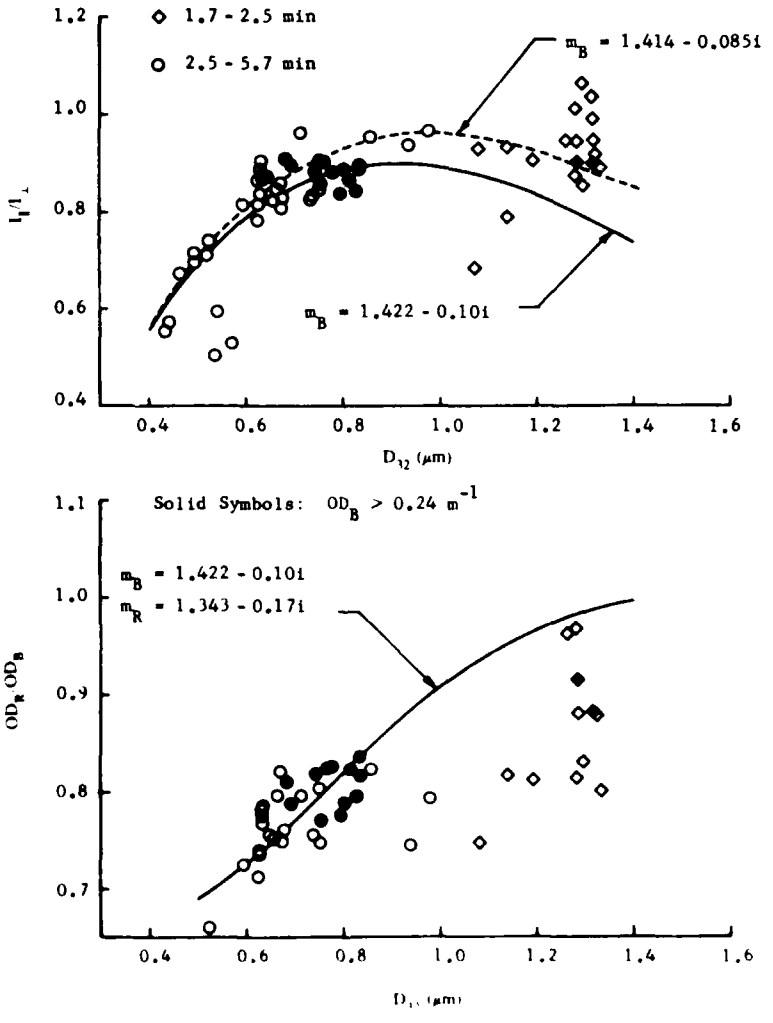

Fig. 13 — Optical density ratios and 90° scattering ratios for nonflaming combustion of chlorinated alkyd paint exposed to a radiant flux of 5 W/cm² in 100°C ventilation air

In order to fit the optical density ratios (OD_R/OD_B) plotted in the lower part of Fig. 13, it was necessary to allow the complex refractive index m to vary with wavelength. A fairly good fit for particles smaller than 0.85 μm was obtained by using $m_B = 1.422 - 0.10i$ (obtained from $I_\parallel/I_\perp$ data) and $m_R = 1.343 - 0.17i$. The theoretical curve obtained with this combination of refractive indices is also shown in the lower plot of Fig. 13.

The curve fits, and data shown in Fig. 13 indicate a strong possibility that moderately absorbing particles are produced by the nonflaming combustion of the chlorinated alkyd paint in air heated to 100°C. Although m_R and m_B are assumed to be constants during the curve fitting process, the actual values probably vary with time during the test; this may account for the scatter of the experimental data values around the theoretical curves. Such refractive index variations would indicate variations in the chemical compositions of the smoke particles during various stages of the pyrolysis process.

Figure 14 shows the particulate volume fractions for the nonflaming tests of the chlorinated alkyd paint samples. The volume fractions for the room temperature test were computed by using the refractive index values given in Fig. 12, which were obtained from the 90° scattering data assuming nonabsorbing particles. The corresponding curve for the 100°C test was obtained by using a constant value of the complex refractive index ($m = 1.422 - 0.10i$ for moderately absorbing particles) determined by the curve-fitting procedure illustrated in Fig. 13. Volume fractions for the 100°C test were also computed assuming nonabsorbing particles; for most of the test these values ranged from 4% to 18% lower than those calculated by using the complex refractive index. The shapes of the curves of volume fraction vs time and their dependence on ventilation air temperature are similar to those of the optical density curves given in Fig. 13. This shows that the optical density of the smoke is determined principally by its concentration and that variations in particle size and refractive index only play secondary roles. Peak volume fractions for these tests are given in Table 5.

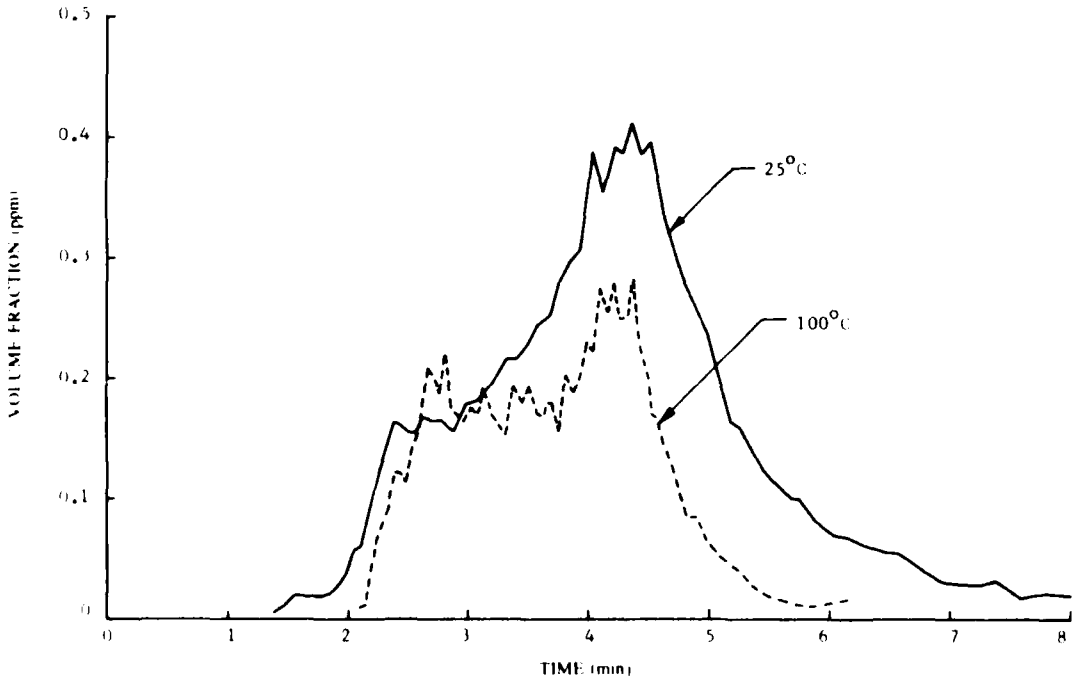

Fig. 14 Effect of ventilation air temperature on the particulate volume fraction for nonflaming combustion of chlorinated alkyd paint exposed to a radiant flux of 5 W/cm^2

For the case of *flaming* combustion of the chlorinated alkyd paint samples, the soot particles produced are highly absorbing, and the determination of the complex refractive index directly from the measured values of OD_R/OD_B and $I_\parallel/I_\perp$ is difficult and unreliable. Figure 15 shows measured values of $I_\parallel/I_\perp$ and OD_R/OD_B plotted vs D_{32} for a typical flaming test of the chlorinated alkyd paint conducted in room temperature air. Also plotted in Fig. 15 are curves of $I_\parallel/I_\perp$ and OD_R/OD_B vs D_{32} which were calculated by using the Mie scattering theory for spheres with m = 1.57−0.56i. The measured values of $I_\parallel/I_\perp$ are seen to cluster about 0.18 which is about 12% below the theoretical values. In addition, the measured optical density ratios lie about 20% below the Mie curve for these smoke particles. Similar discrepancies between theoretical and measured values of $I_\parallel/I_\perp$ and OD_R/OD_B were also obtained for flaming tests conducted in heated ventilation air.

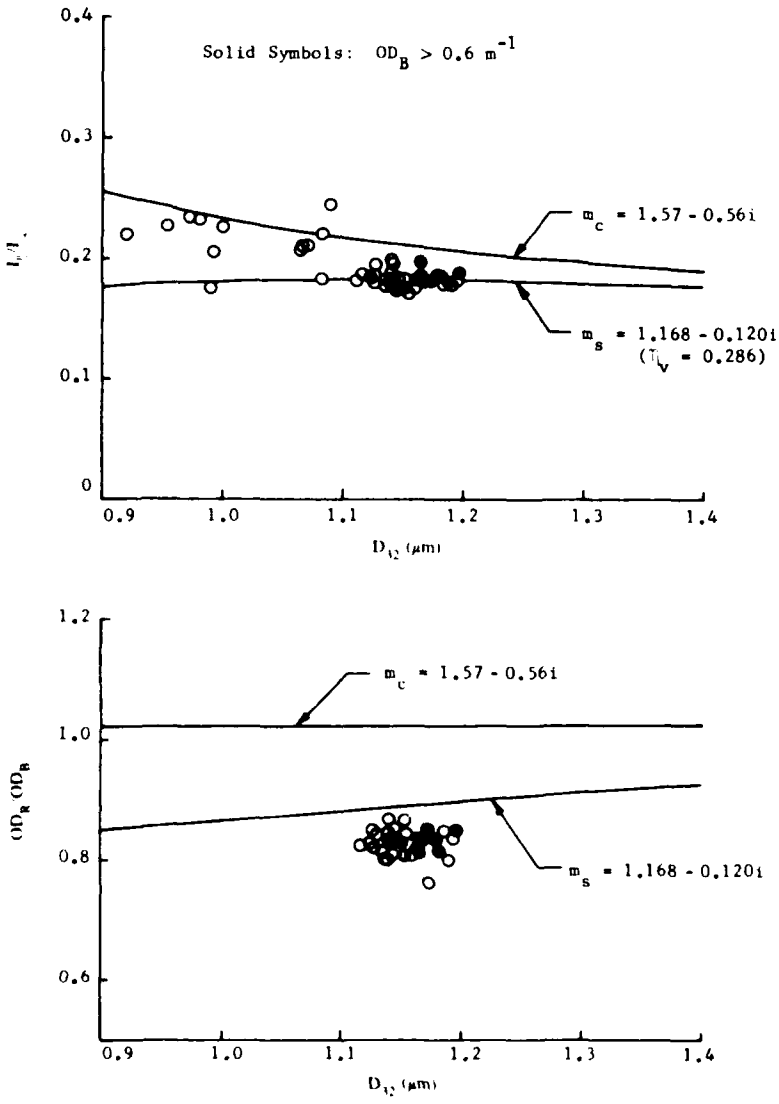

Fig. 15 — Optical density ratios and 90° scattering ratios for flaming combustion of chlorinated alkyd paint exposed to a radiant flux of 5 W/cm² in room temperature ventilation air (25°C)

In a recent paper by Santoro et al. [11] it was shown that similar discrepancies between experimental observations and the Mie theory for polydispersions of absorbing spheres can be resolved. There it was concluded that the loosely packed, low-density soot agglomerates have an effective refractive index m_s that is significantly reduced below the refractive index of the particulate material m_c of which they are composed. This downward scaling of the refractive index was applied to the interpretation of the data shown in Fig. 15 by using the Lorentz-Lorenz formula to relate m_s and m_c as a function of η [11,12] the fraction of the optical mean "particle" volume that is actually occupied by the particulate material. By using $m_c = 1.57 - 0.56i$, measured values of $I_\parallel/I_\perp$ and D_{32} yield a unique value of $m_s = n_s - ik_s$ from which η_v can also be determined. The best fit to the $I_\parallel/I_\perp$ data shown in Fig. 15 is given by $m_s = 1.168 - 0.120i$ for which $\eta_v = 0.286$. By using this same value of m_s, the Mie theory gives significantly lower values of OD_R/OD_B, which are only about 7% above the experimental data (Fig. 15). Although this small remaining discrepancy may be due to part to variations in the effective refractive index with wavelength, it is also within the expected experimental error.

Effective refractive indices were also obtained from the flaming tests in heated ventilation air; these are given in Table 5 along with the corresponding values of η_v. For these tests, values of η_v were between 0.24 and 0.30 with the largest values occurring at 100°C; however, the effect of environmental temperature upon η_v appears to be weak. Therefore, for all of the flaming tests of the chlorinated alkyd paint, an average value of $\eta_v = 0.264$ was obtained for which the corresponding effective refractive index is $m_s = 1.155 - 0.110i$. Thus the soot particulates produced by flaming combustion of the chlorinated alkyd paint appear to be very loose, low-density aggregates of smaller primary soot particles that occupy slightly more than 25% of the optical mean volume as determined from the forward scattering measurements. The effective complex refractive index of these agglomerates (both n_s and k_s) is much smaller than the complex refractive index customarily used for the bulk particulate material.

Volume fractions for flaming combustion of the chlorinated alkyd paint samples were calculated by using the downward scaled complex refractive index m_s values given in Table 5. These curves for ventilation air temperatures of 25°, 100°, and 300°C are presented in Fig. 16 where the data has been corrected to the standard flow rate of 425 l/min to eliminate the dilution effect at high temperatures. The peak volume fractions are also given in Table 5; these values exhibit the same trend with increasing ambient temperature as the optical density. Again smoke concentration appears to be the primary factor influencing the light-obscuring properties of the smoke produced by flaming combustion of this material. For comparison, volume fractions were also computed based on the complex refractive index, $m_c = 1.57 - .56i$, of the bulk particulate material. Significant differences in the calculated volume fractions were found; peak values obtained by using the bulk refractive index averaged about 17% lower than those determined by using the effective refractive index.

Values of the total particulate volume were obtained by integrating the volume fraction curves in Figs. 14 and 16 with respect to time. These values were then normalized by dividing by the unburned sample weight to yield a specific total particulate volume (i.e., total particulate volume per unit mass of material burned). Values of the specific total particulate volume (STPV) for both flaming and nonflaming modes are also given in Table 5. For *nonflaming* combustion, the STPV, like the peak volume fraction, decreases markedly as the ambient temperature is increased. At 100°C the STPV is less than half of that obtained at room temperature. On the other hand, for flaming combustion of the chlorinated alkyd paint samples, the STPV is rather insensitive to the ventilation air temperature as seen from Table 5. The average STPV value obtained for all of the flaming tests is nearly 0.05 cm^3/g. This result is surprising considering the much stronger effect of temperature on the peak height and shape of the curves of volume fraction vs time; however, a close inspection of the curves shown in Fig. 16 reveals that the area under each of the three curves is roughly the same.

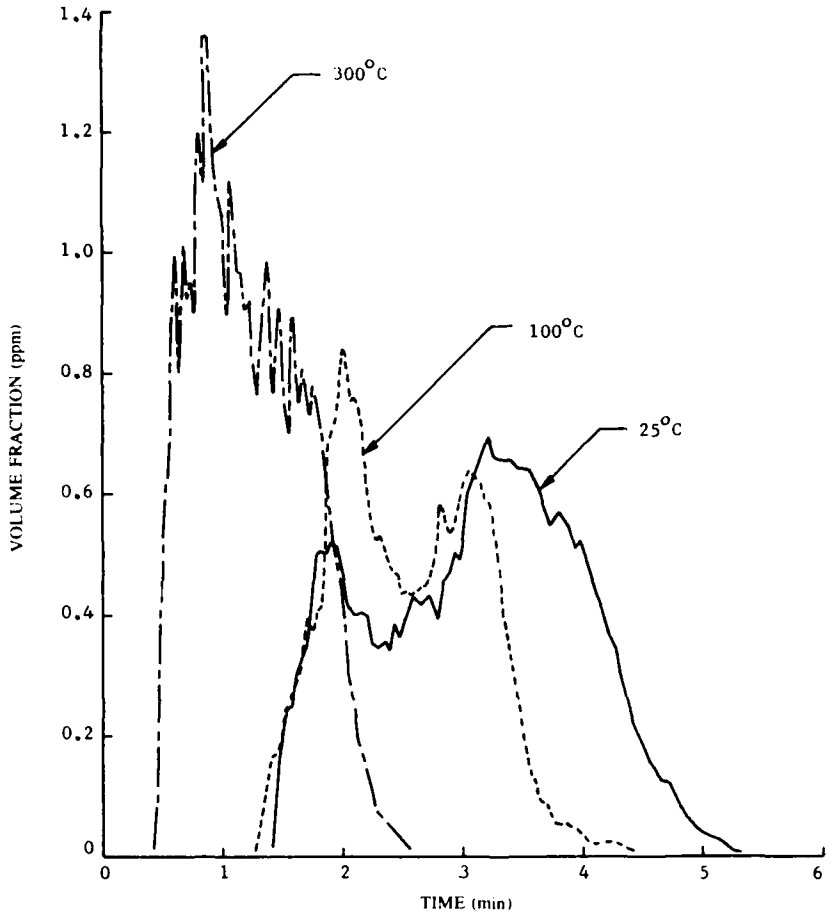

Fig. 16 — Effect of ventilation air temperature on the particulate volume fraction for flaming combustion of chlorinated alkyd paint exposed to a radiant flux of 5 W/cm^2

Although no sampling data were available for elevated temperatures, the effect of ambient temperature on Γ was estimated from the optical data. These data are also given in Table 5 for both flaming and nonflaming combustion, where Γ is normalized with respect to the corresponding room temperature value. The Γ values for the nonflaming combustion mode follow the same trend with increasing ventilation air temperature as the specific total particulate volume. For flaming combustion, however, the Γ values estimated for the tests conducted at 100°C and above are all roughly 75% of the corresponding room temperature value.

With the assumption of a particulate density $\rho_p = 1.3$ g/cm^3 for smoke particles produced by nonflaming combustion and $\rho_p = 2.0$ g/cm^3 for soot produced by flaming combustion, the total particulate mass was estimated from the optically determined total particulate volume. For the room temperature tests, the optically determined values of the total particulate mass were then compared with the corresponding values estimated by particulate sampling. For nonflaming combustion, assuming spherical particles, the optically determined particulate masses were about 2.5 times as large as the particulate masses estimated by sampling. Similar discrepancies have been obtained with previously tested materials such as PVC-nitrile rubber and PVC cable jacket material [4]. Possible sources of this discrepancy are the uncertainties in the particulate density and complex refractive index, losses

in the sampling system, and departures of the size distribution from that assumed in reducing the optical data. For flaming combustion, the total particulate mass was estimated from the optically determined particulate volume obtained by using the downward scaled (effective) refractive index by multiplying it by the factor η_v, which represents the fraction of the optical volume occupied by the particulate material. The total particulate masses obtained in this manner average about 3.8 times larger than the corresponding masses obtained by particulate sampling. However, when the refractive index of the bulk particulate material (i.e., $m_c = 1.57 - 0.56i$) is used and the η_v correction is not applied (i.e. the particles are assumed to be compact spheres), the discrepancy between the total particulate masses is much larger. Here, the optical particulate mass averages about 11.6 times the mass obtained by sampling. This latter discrepancy is consistent with previous results for flaming tests of PVC-nitrile rubber, PVC cable jacket, and hydraulic fluid [4] in which refractive index downscaling and η_v corrections were not used. It appears from the above results that the nonspherical shape and high void fraction typical of soot agglomerates obtained during flaming combustion accounts for most of the particulate mass discrepancy, while the remaining discrepancy is probably due to the same effects as noted above for nonflaming combustion.

The STPV values given in Table 5 can be used to estimate the smoke volume concentration and optical density for a known quantity of chlorinated alkyd paint burning in a confined space. The STPV value is first multiplied by the total mass of dry paint originally present in the compartment to obtain the total volume of the smoke particulates produced during combustion. Assuming that all of the smoke is uniformly distributed throughout the compartment, the volume fraction φ is next obtained by dividing the previous result by the compartment volume. To obtain the optical density the following formula is used:

$$OD_B = 0.651\ \bar{Q}_{ext}(D_{32}, m_B)\ \varphi/D_{32}$$

where D_{32} is obtained from Table 4, m_B (effective) is obtained from Table 5, and $\bar{Q}_{ext}$ is calculated by using the Mie scattering theory. As an example, consider a 3.04 × 3.04-m (9.29 m^2) (10 × 10-ft) bulkhead covered with 5 coats of chlorinated alkyd paint (approximately 2 kg/m^2) burning in a 708-m^3 (25,000-ft^3) space. The weight of the unburned polymer in this case is 18.6 kg. From Table 5 the worst nonflaming case occurs for a 5.0 W/cm^2 radiant flux in room temperature air, for which the STPV is about 0.040 cm^3/g, while only slightly more particulates (0.050 cm^3/g) are produced for a typical flaming case that occurs in 25° to 300°C air. The worst case values of optical volume fraction are 1.05 ppm for nonflaming combustion and 1.31 ppm for flaming combustion, while the corresponding values of optical density (blue) are 2.7 m^{-1} and 1.4 m^{-1} respectively. From this example, it is clear that greater light obscuration occurs under nonflaming conditions than for flaming combustion. For the nonflaming case, the light attenuation is severe, amounting to about 0.2% of the incident light transmitted over a 1-m optical path length. It is unlikely that such large amounts of the chlorinated alkyd paint will undergo nonflaming combustion in an actual fire, however, since the radiant flux would have to be supplied by flaming combustion of neighboring materials. Thus, flaming combustion of the paint would be expected to occur, especially if the ambient temperature rises above 200°C. In this case the light obscuration is much less severe, amounting to a 4% transmission of blue light over a 1-m optical path length.

SMOKE PHYSICAL PROPERTIES DATA FOR INTUMESCENT PAINT

Description of Material and Sample Preparation

The intumescent paint tested was No. 9788 Fire Retardant Paint that is manufactured by Ocean Chemical Co. of Savannah, Georgia specifically for marine applications. Upon exposure to heat or flame this paint swells rapidly to form a thick porous char that insulates and protects the substrate

from the fire environment. The Ocean 9788 intumescent paint is an oil-based material that is about 70% solids by weight. It has a wet density of 1.222 g/cm^3, and it dries to form a film with a density of 1.673 g/cm^3. The chemical composition of this paint is proprietary and thus was not available. The color of the paint used in these tests was white.

Samples of the Ocean 9788 intumescent paint were prepared by brushing it onto 5.1-cm squares (2 in.) of cold rolled steel substrate 1.19-mm (3/64-in.) thick. The average weight of the substrates was 29.5 g. The substrates were first cleaned with acetone, then 3 liberal coats of paint were applied with a small brush over a 12-day period with a 1-day drying time between the first and second coats. The average dry mass of paint applied in this manner was 1.63 g with a standard deviation of 0.14 g. This yields an average dry film thickness of 0.378 mm (0.015 in), which is close to the recommended thickness. Storage time under ambient laboratory conditions for these samples ranged from 7 to 56 weeks.

One of the samples was exposed to the flame of a Bunsen burner to observe the intumescent behavior. After about 20 to 30 s of heating in the flame, the paint began to darken and blister, followed by rapid vertical swelling and expansion of the char. This was accompanied by a slight lateral contraction. The char thickness ranged from about 22 mm in the center to about 27 mm along one edge. The surface had a nodular texture with a scale of about 2 mm. Cutting into the char revealed a fragile cellular structure—light, dry, and brittle in the outer layers and somewhat tacky in the layers adjacent to the substrate.

Tests in Room Temperature Ventilation Air

Tests of the Ocean 9788 intumescent paint were conducted in room temperature ventilation air (25°C) with a radiant flux of 5 W/cm^2. Tests were run either with a propane pilot flame or without to study the smoking behavior of the paint under both flaming and nonflaming modes of combustion. However, owing to the fire retardant nature of this paint, flaming combustion never occurred in the room temperature tests. Therefore, all of the room temperature tests were essentially conducted under nonflaming conditions with only slight differences owing the presence of the small propane pilot flame. For all of these tests the ventilation air flow rate was 142 l/min (5 ft^3/min). The results of these tests are presented in Figures 17 through 20 and Tables 6 and 7.

For the intumescent paint samples it was impossible to obtain weight loss data during the test because of disturbances caused by the rapidly swelling char that contacted the pilot burner tube and its igniter wire. However, an average mass loss rate was calculated based on the initial and final weights and the time interval over which significant quantities of smoke were being evolved (based on optical density measurements). For the room temperature tests, this average mass loss rate ranged from 0.05 to 0.08 mg/cm^2-s (Table 6). The mass of the char residue, expressed as a percentage of the initial sample mass, was also obtained for the room temperature tests. These values (Table 6) ranged between 55% (with pilot flame) and 58% (no pilot flame). Figure 17 shows the black char residues obtained in the room temperature tests of the intumescent paint. The coarsely nodular, porous surface texture of the thick char layer is readily seen in these photographs. The white patch near one edge of the char obtained in the test with the pilot flame was caused by direct impingement of the pilot flame upon the char, burning off some of the carbonaceous material and leaving a white residue.

Smoke particle size distributions were obtained by using the cascade impactor for room temperature nonflaming tests of the Ocean 9788 intumescent paint exposed to a 5 W/cm^2 radiant flux both with and without the pilot flame. Figure 18 shows these size distributions as cumulative curves generated by plotting the percentage of particulate weight having particle diameters less than a given particle size vs. the particle size on log-normal probability coordinates. In both cases, a straight line gives a good fit to the cascade impactor data (plotted points), which indicates that the size distribution is log-normal. Table 7 gives mass median diameters D_{MMD} and standard deviations σ_g obtained from

Table 6 — Sample Weight Loss Data for Intumescent Paint on Steel Substrate

Mode	Ventilation Air Temperature (°C)	Radiant Flux (W/cm^2)	Average Mass Loss Rate (mg/cm^2-s)	Char Residue (Percent of Initial Weight)
Nonflaming	25	5.0	0.050	57.8
Nonflaming	100	5.0	0.19	54.9
Nonflaming	150	5.0	0.21	52.5
Nonflaming	200	5.0	0.84	56.4
Nonflaming	300	5.0	—	50.8
Nonflaming[a]	25	5.0	0.081	55.1
Nonflaming[a]	100	5.0	0.28	54.8
Nonflaming/flaming	100	5.0	0.12	56.4
Nonflaming[a]	300	5.0	0.3	44.7
Nonflaming/flaming	300	5.0	0.24	45.5

[a]Pilot burner on, but no flaming ignition.

Table 7 — Smoke Properties Data for Intumescent Paint

Mode	T (°C)	Radiant Flux (W/cm^2)	Γ	D_{MMD} (μm)	σ_g	OD_{max} Blue	(m^{-1}) Red	D_{32}^a (μm)	Time to Peak OD (min)
Nonflaming	25	5.0	0.11	0.61	1.96	0.57	0.42	0.70	3.4
Nonflaming	100	5.0	—	—	—	0.71	0.61	0.80	3.0
Nonflaming	150	5.0	—	—	—	0.40	0.33	0.50	3.0
Nonflaming	200	5.0	—	—	—	0.14	0.06	0.63[b]	2.2
Nonflaming	300	5.0	—	—	—	<0.10	<0.10	c	—
Nonflaming[d]	25	0.5	0.09	0.39	2.06	0.45	0.32	0.58	4.0
Nonflaming[d]	100	5.0	—	—	—	0.30	0.18	0.73	3.0
Flaming	100	5.0	—	—	—	0.13	0.11	1.18	4.8
Nonflaming[d]	300	5.0	—	—	—	0.48[e]	0.25[e]	c	1.6
Flaming	300	5.0	—	—	—	0.08	—	1.34[b]	4.3[b]

[a]Average of data points near OD_{max}.
[b]At peak scattering rather than OD_{max}.
[c]No measurable scattering in one or both angles.
[d]Pilot burner on, but nonflaming mode.
[e]Narrow peak without corresponding scattering.

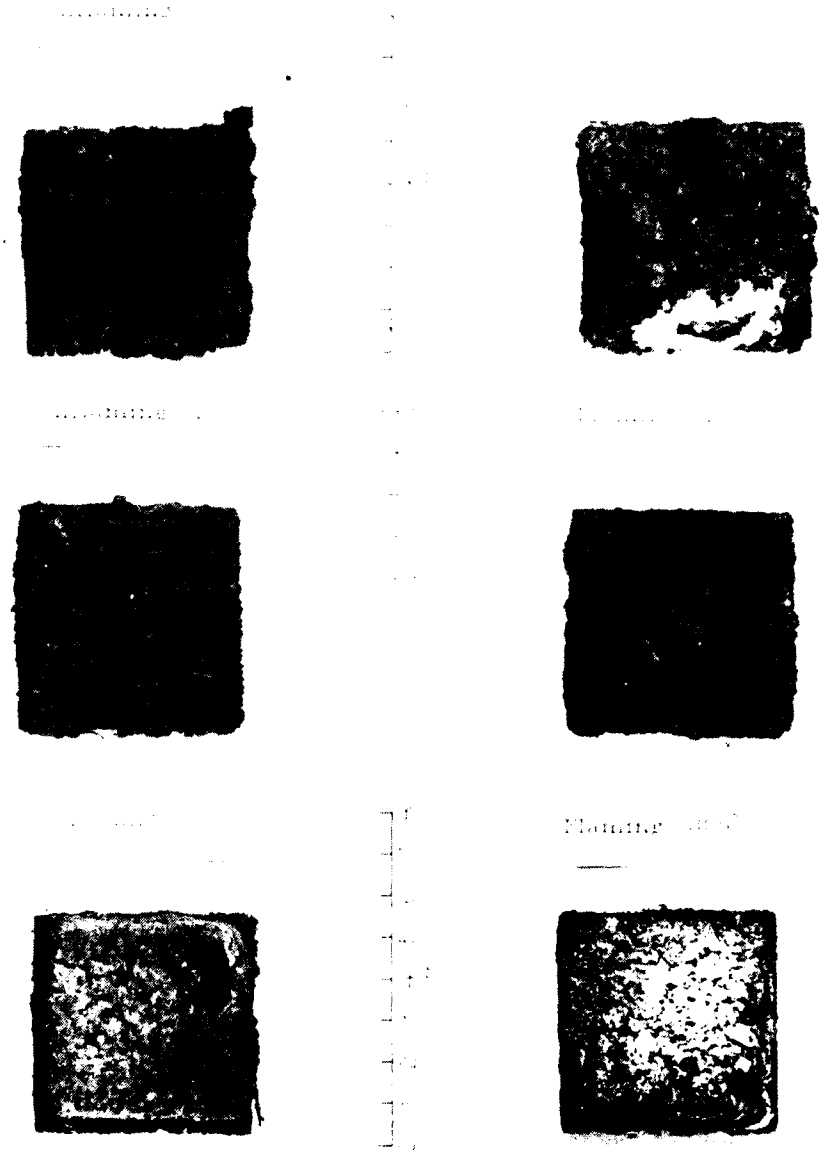

Fig. 17 — Char residues for intumescent paint tests

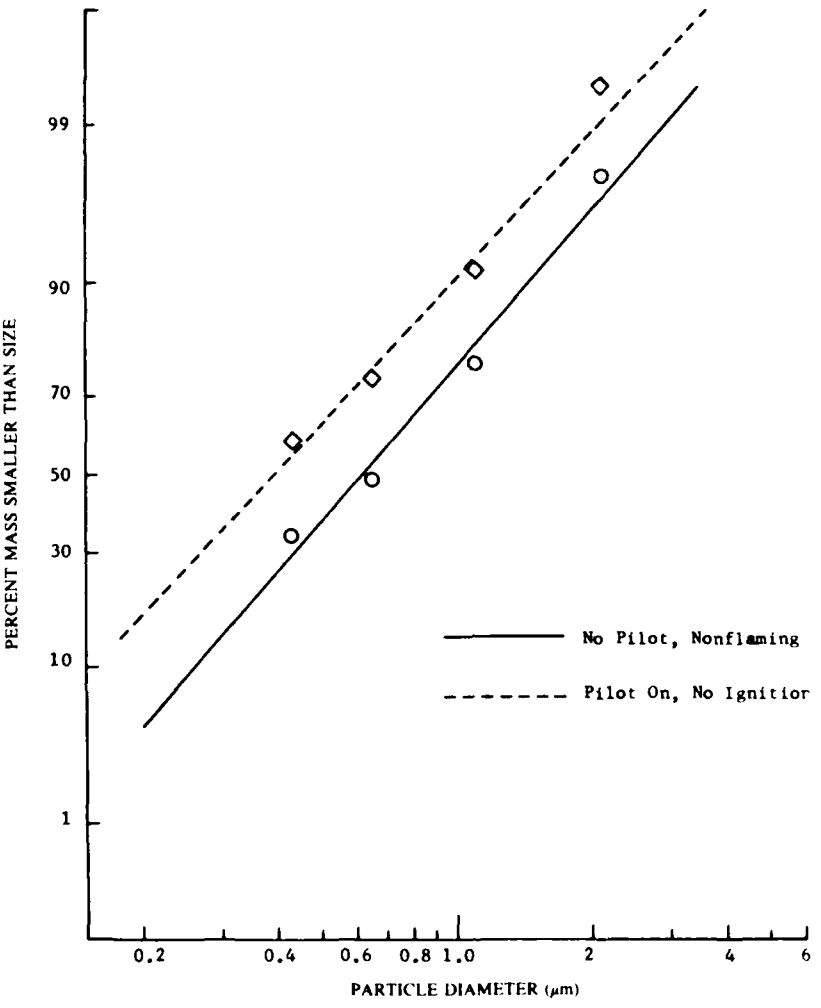

Fig. 18 — Smoke particle size distribution for nonflaming combustion of intumescent paint exposed to a radiant flux of 5 W/cm^2 in room temperature ventilation air (25°C)

these curves. For nonflaming combustion without the pilot flame, the particulates consist of a mixture of white and light tan or beige solid particles with a $D_{M(3)}$ of about 0.6 μm. Here the total mass of particulates collected on the cascade impactor was only 6.6 mg (0.43 to 2.1 μm), while about 3.5 mg were collected on the absolute filter ($\leq$ 0.43 μm). The particles collected on the cascade impactor plates were examined under a microscope at 30X; they appeared as small agglomerates (about 1 mm across) of fine, white, solid particles. The sample on the filter appeared to consist of a fine light tan or beige powder. For the test conducted with the pilot flame, flaming ignition did not occur, but a $D_{M(3)}$ of only about 0.4 μm was obtained. Here the total mass of particulates collected was only 9.8 mg, approximately 59% of which was collected on the absolute filter ($\leq$ 0.43 μm). The visual appearance of the particulates collected was the same as the case without the pilot flame.

The sampling data was also used to determine the fraction of the sample mass loss converted to particulates (F) for the room temperature tests. These values of F, which are given in Table 7, show that between 9% and 11% of the total mass loss appears as particulates for nonflaming combustion of the Ocean 9788 intumescent paint under 5 W/cm^2 radiant flux.

The in situ optical system was used to obtain the mean particle diameters D_{32} and the optical densities produced by nonflaming combustion of the intumescent paint samples. A comparison of mean particle sizes obtained with a radiant flux of 5 W/cm^2, both with and without the pilot flame, is given in Fig. 23, while the corresponding optical densities are given in Fig. 20.

Figure 19 shows that for nonflaming combustion of the Ocean 9788 intumescent paint a sharp peak in smoke mean particle size occurs shortly after pyrolysis begins. For the case without the pilot flame, the maximum value of D_{32} is about 1.3 μm, while D_{32} peaks at about 1.1 μm when the pilot flame is lit. In both cases, smoke mean particle size decreases rapidly during the next 2 min and then levels off to relatively constant values between 0.6 and 0.7 μm for the remainder of the test. Although the pilot flame does not initiate flaming combustion in these room temperature tests, it has a small effect on mean particle size as evidenced by the slightly smaller values of D_{32} obtained with the pilot flame on. Perhaps this is due to a small fraction of the smoke particulates that pass directly through the pilot flame and experience some degree of evaporation or combustion.

Figure 20 presents the smoke optical densities at the blue green argon line (0.488 μm) for nonflaming combustion of the intumescent paint samples in 25°C ventilation air. Here the optical density rises rapidly between 2 and 3 min after initiation of radiant exposure and reaches a modest peak of about 0.5 to 0.6 m^{-1} lasting about 1 min. Thereafter, a much slower decline in light obscuration occurs. For the case with the pilot flame, the optical densities are slightly smaller, which is consistent with the smaller mean particle size.

A comparison of Figs. 19 and 20 reveals that the sharp D_{32} peak occurs while the optical density is very low, which implies that the number density and volume fraction of these larger particles is relatively small. These curves also show that as the optical density is rapidly increasing, the mean particle diameter is rapidly decreasing, and the peak optical density occurs just as D_{32} is leveling off to a nearly constant value. Table 7 gives values of D_{32} corresponding to the peak optical densities. These optical D_{32} range from 15% (no pilot) to 50% (with pilot) larger than the corresponding $D_{32(c)}$ obtained by cascade impactor sampling. Aside from experimental errors, part of this discrepancy may be due to nonspherical shape of the solid particles generated by nonflaming combustion of the paint.

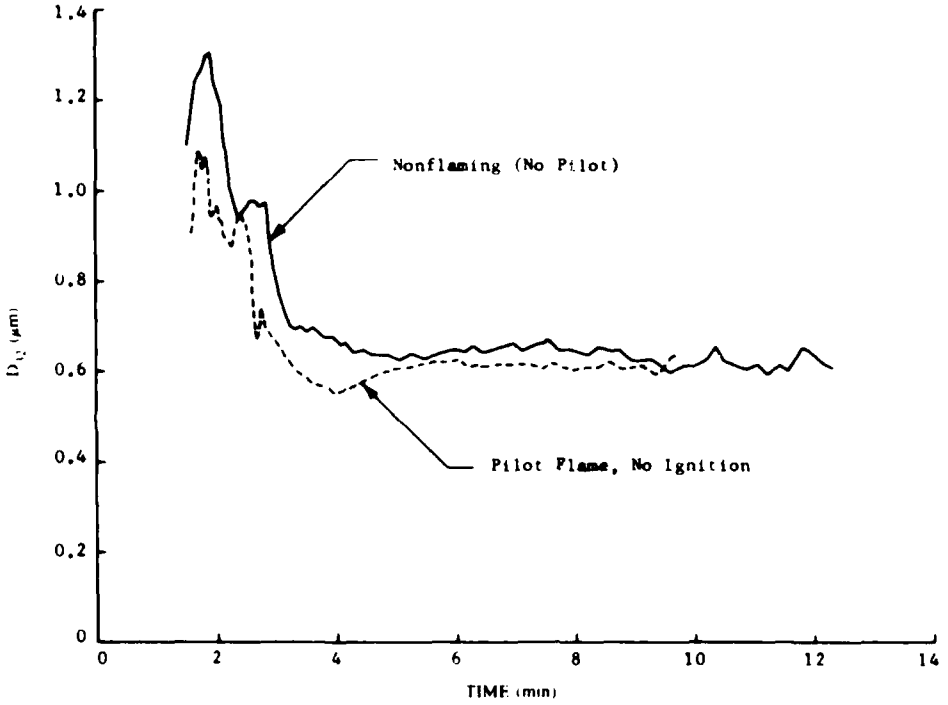

Fig. 19 Smoke mean particle diameters for nonflaming combustion of intumescent paint exposed to a radiant flux of 5 W/cm² in room temperature ventilation air (25°C).

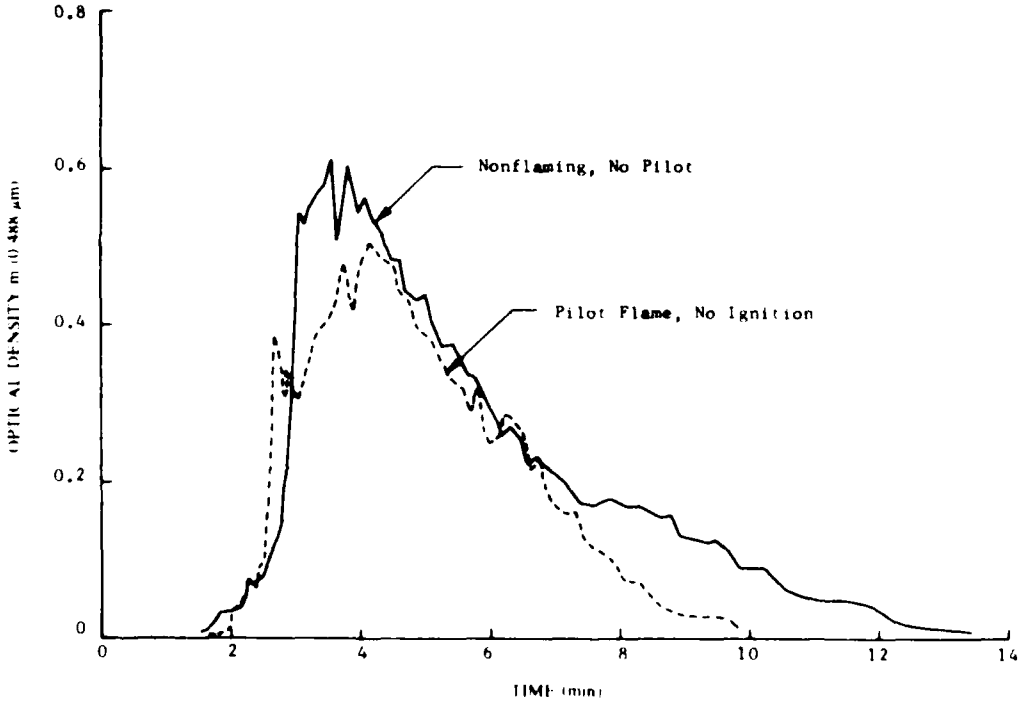

Fig. 20 Smoke optical densities for nonflaming combustion of intumescent paint exposed to a radiant flux of 5 W/cm² in room temperature ventilation air (25°C).

Tests in Heated Ventilation Air

A series of tests in heated ventilation air was conducted for the Ocean 9788 intumescent paint samples both with and without the pilot flame. For the nonflaming tests (no pilot flame), data were obtained at ventilation air temperatures of 100°, 150°, 200°, and 300°C. For high temperature tests with the pilot flame, the ventilation air was heated to 100° and 300°C. For these last two test conditions, a brief period of flaming combustion was usually observed. The results of these tests are presented in Figs. 17, 21 to 24, and Tables 6 and 7.

As seen in Table 6, increasing the ventilation air temperatue under nonflaming conditions from 100° to 150°C increased the average mass loss rate by a factor of four, while a further increase in air temperature to 200°C yielded another fourfold increase in average mass loss rate. With the exception of the 200°C test, increasing the ventilation air temperature (25° to 300°C) for nonflaming conditions resulted in a small but steady decrease in the percentage of initial mass remaining as char. For tests with the pilot flame, average mass loss rate again increases with air temperature, but the amount of increase is considerably less than in the nonflaming tests. This is opposite to what is expected, since the pilot flame and any flaming combustion of pyrolysate gases should increase the heat transfer to the polymer surface resulting in greater mass loss rates. However, the errors incurred in estimating the average mass loss rate in the absence of instantaneous weight loss data are expected to be significant and may account for this discrepancy. For the 300°C tests with the pilot flame the amount of char remaining is considerably less (about 45%) than for the corresponding nonflaming test (about 51%).

Char residues obtained from the high temperature tests of the Ocean 9788 intumescent paint are also shown in Fig. 17. For the nonflaming tests there are considerable variations in the thickness and surface topography of the char layers, but there appears to be little correlation of these variations with temperature. These variations in char appearance are probably due to variations in some other factor such as paint film thickness, age of sample, or humidity of ventilation air. On the other hand, for cases in which flaming combustion occurred, the chars obtained exhibited definite characteristic features. In the locations on the surface where flamelets were observed, the char was much darker than the surrounding surface. In some cases the intumescence was enhanced by the localized flamelets to produce columnar features, the largest such char column observed was about 15 mm in diameter and about 7 mm high. In addition, a moderate coating of white material covered most of the surface that had the same nodular texture as in the nonflaming tests.

Particle size and optical density data obtained from tests of Ocean 9788 intumescent paint samples conducted in hot ventilation air are shown in Figs. 21 and 22 for nonflaming combustion and in Figs. 23 and 24 for flaming combustion. In the figures for nonflaming combustion the room temperature data are also shown for comparison, however, this could not be done for flaming combustion since flaming ignition never occurred in the room temperature tests. High temperature data are also given in Tables 6 and 7. In all flaming tests a small propane pilot flame was maintained over the sample throughout the test, and the radiant flux was 5 W/cm^2 for all tests.

Figure 21 shows the effect of increasing the ventilation air temperature on mean smoke particle diameter D_{32} for nonflaming tests of the intumescent paint. For tests at 100° and 150°C the curves of D_{32} vs time are qualitatively similar to that for the room temperature test, but the particle sizes obtained during the last half of the 10 min exposure period (where D_{32} is nearly constant) are somewhat smaller for the higher temperature tests (about 0.5 μm). Furthermore, there is a pronounced dip in the D_{32} curve to about 0.3 μm for the 150°C test (t = 3.5 min) that does not appear at the lower temperatures. For the 200°C test, measurable quantities of smoke particulates were obtained only for a very brief period, about 2 min after initial exposure, during which D_{32} dropped rapidly from about 0.9 to 0.4 μm. At each temperature, the largest particles occurred in the initial stages when the optical density was low. For the test conducted at 300°C without the pilot flame, no light scattering or

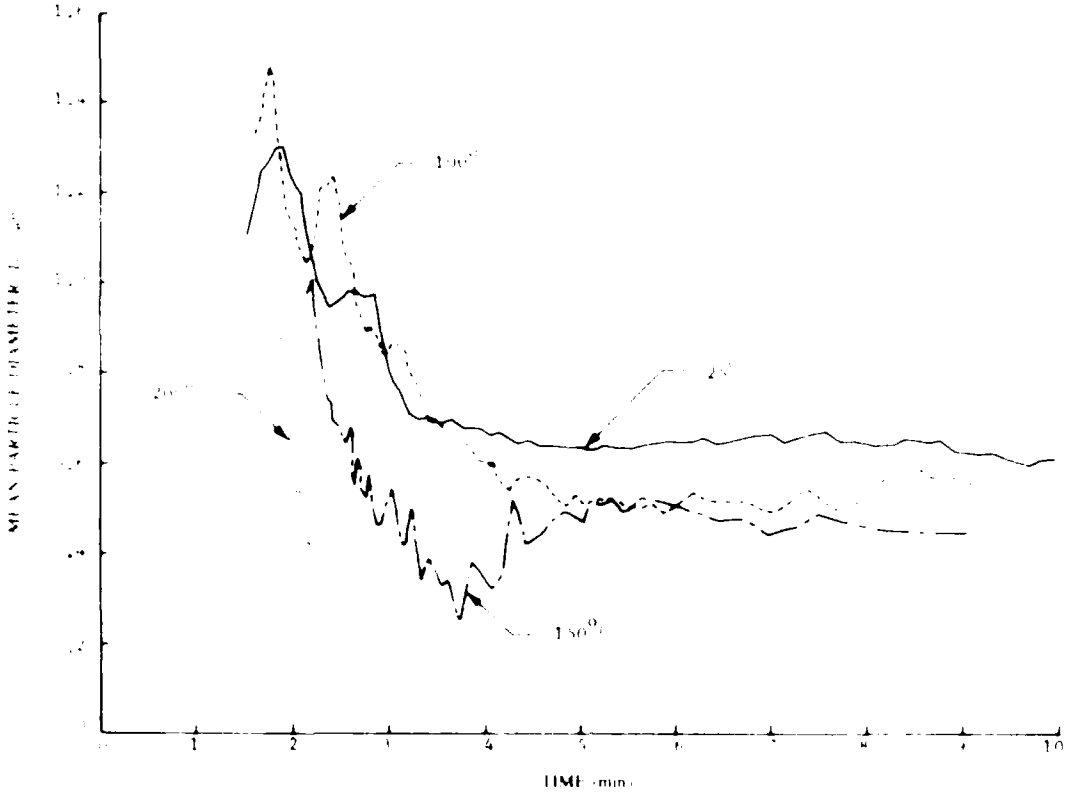

Fig. 21 Effect of ventilation air temperature on the smoke mean particle diameter for nonflaming combustion of intumescent paint exposed to a radiant flux of 5 W/cm².

absorption by smoke particulates was detected. Table 7 shows that for ambient temperatures of 25 to 150°C, the value of D_{32} at the time of maximum optical density ranges from 0.5 to 0.8 μm.

Figure 22 presents the effect of ventilation air temperature on smoke optical density (0.488 μm wavelength) for nonflaming combustion of the intumescent paint. Increasing the ambient temperature is seen to have a dramatic effect on optical density. At 100°C the peak in optical density is considerably higher and occurs earlier than at room temperature, and the decline in optical density following the peak is much more rapid at the higher temperature. In contrast, further moderate increases in ambient temperature greatly reduce the peak optical density and the time interval during which measurable light obscuration occurs. Part of this reduction in optical density shown in Fig. 22, which gives directly measured values, is due to the increased dilution of the smoke particulates by the higher volumetric flow rate of the heated ventilation air (Table 1). The values of peak optical density given in Table 7 have been corrected for this effect; they reflect more accurately the decline in smoke production as the ambient temperature is raised above 100°C.

The effect of increasing temperature on optical density as shown in Fig. 22 and Table 7 is probably due to the combined effects of increased pyrolysis rate and reduced condensation of pyrolysate vapors. Increasing the ambient temperature from 25° to 100°C apparently accelerates the pyrolysis reactions without significantly reducing the condensation process that produces particulates, thus the peak optical density increases and the width of the peak narrows. This indicates that the boiling point of the particulates exceeds 100°C. The dramatic reduction in optical density obtained with increases in temperature above 100°C indicates that suppressed condensation of pyrolysis vapors is then the dominant factor. Thus, most components of the smoke particulates produced by nonflaming combustion of the intumescent paint probably have boiling points between 150° and 200°C. The absence of

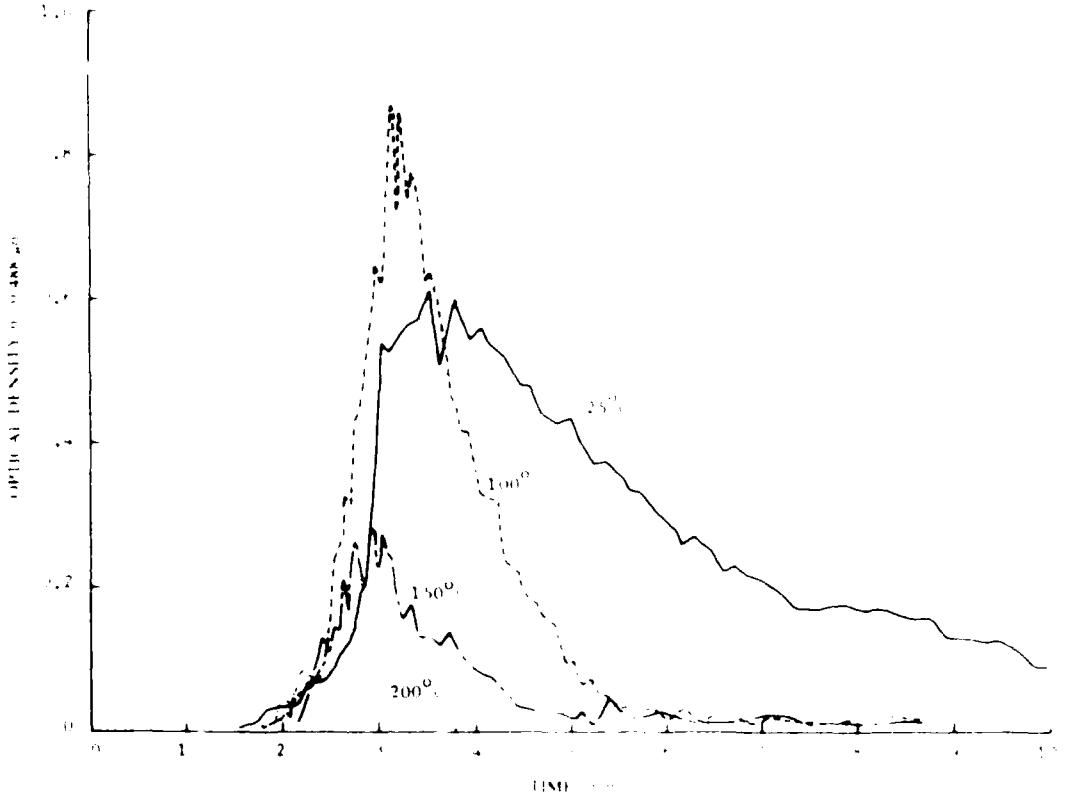

Fig. 22 — Effect of ventilation air temperature on the smoke optical density for nonflaming exposure of intumescent paint exposed to a radiant flux of 5 W/cm²

measurable smoke particulates at temperatures above 300°C indicates that virtually none of the components of the smoke particulates has a boiling point exceeding 300°C. This eliminates the possibility that the solid particles collected by cascade impactor sampling and filtration consist of inorganic pigment materials that have much higher vaporization temperatures.

At elevated ambient temperatures it was possible, under certain conditions, to obtain *flaming* combustion of the Ocean 9788 intumescent paint. Figures 23 and 24 give the results of three tests conducted in 100°C ventilation air in which the propane pilot flame was used. In Test A, flaming ignition did not occur; in Test B, nonflaming smoke was detected shortly after 1 min, and flaming ignition occurred about 2 min later; in Test C, the smoking behavior of the paint sample was similar to Test B, but the onset of pyrolysis and flaming ignition were both delayed by about 2 min.

Figure 23 shows the variations of mean smoke particle diameter with time during these flaming tests. The variation in D_{32} during the initial nonflaming phase is similar to that observed in similar tests conducted without the pilot flame (Fig. 21). The onset of flaming combustion is marked by a sudden increase in D_{32} from 0.5 to 0.6 μm (nonflaming) to about 1.2 μm. This is also accompanied by a sudden decrease in the 90° scattering ratio I/I_o to the low values consistent with the highly absorbing, black, soot agglomerates produced by flaming combustion. For Test B, the flaming phase lasted about 2 1/2 mins. Visual observations during these tests indicated that flaming combustion was intermittent or flickering and was highly localized to specific regions of that sample surface.

Figure 24 shows the optical density variations (0.488 μm wavelength) for the same three 100°C tests. These curves show that the optical density for Test B declined rapidly shortly after flaming ignition, while a low peak was obtained after ignition in Test C. In both tests the optical density observed during flaming combustion was about half of the obtained during the earlier nonflaming phase.

Three tests were conducted in 300°C ventilation air with the pilot flame lit. As in the 100°C tests, brief periods of localized intermittent flaming combustion accompanied by light soot production were observed. In only one of these tests, however, were the light scattering and attenuation signals from this soot sufficiently strong to yield values of mean smoke particle size and optical density. In this test (Table 7), the D_{32} measured at peak scattering was somewhat larger than that obtained at 100°C, while the peak optical density obtained at 300°C was considerably less than that observed at 100°C. These tests also indicate that the duration and extent of flaming combustion of the Ocean 9788 intumescent paint is considerably less at high ambient temperature (300°C) than at intermediate ambient temperature (100°C). This behavior is quite different from the chlorinated alkyd paint for which spontaneous ignition occurs at elevated ambient temperatures. These differences are probably due to the complex physical and chemical processes involved in the intumescence and pyrolysis of the Ocean 9788 paint.

Smoke Particle Refractive Index and Volume Fraction

For *nonflaming* tests of the Ocean 9788 intumescent paint, measurement of the ratio of optical densities, OD_g/OD_B, and the 90° scattering ratio I/I_o were used to estimate the complex refractive index of the smoke particles. Values of the refractive index determined from these measurements under the assumption of nonabsorbing particles for these tests were often lower than expected for smoke particles (less than 1.3), which usually indicates that the smoke particles absorb as well as scatter light ($k > 0$). Thus, the curve fitting technique that was used in determining the complex refractive index for smoke particles produced in tests of the chlorinated alkyd paint in heated ventilation air was also used to determine the refractive index n and absorption index k for smoke produced by the intumescent paint. For each of the nonflaming tests, measured values of I/I_o and OD_g/OD_B were plotted vs D_{32}. Values of n and k were then estimated from the Mie theory curve that best fits the plotted data.

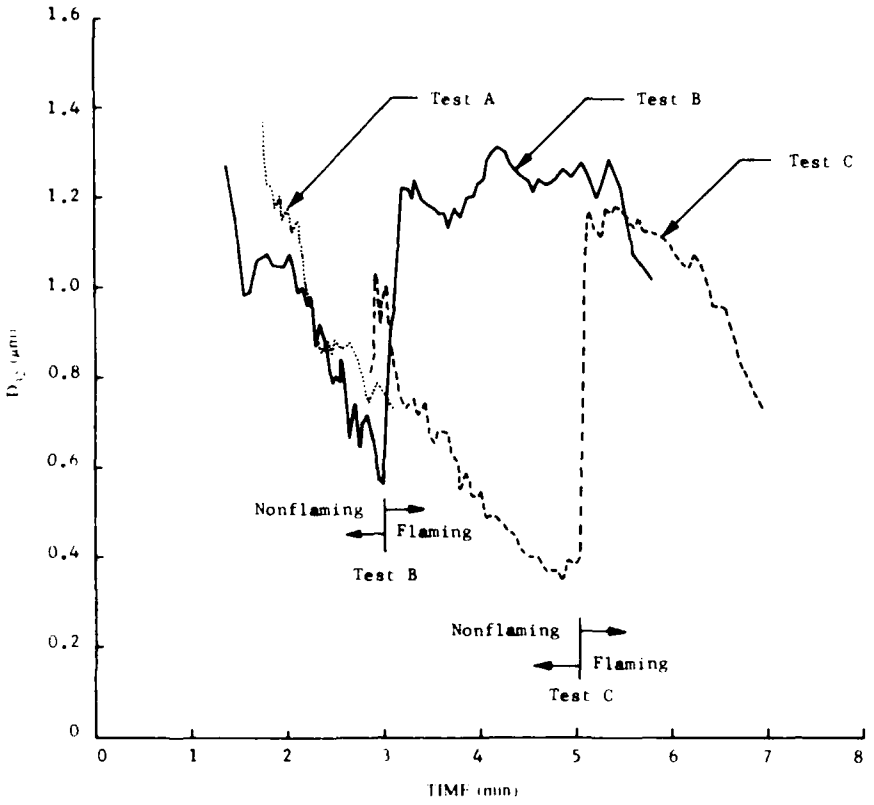

Fig. 23 — Smoke mean particle diameters for flaming combustion of intumescent paint exposed to a radiant flux of 5 W cm^{-2} with pilot flame in heated ventilation air at 100 C

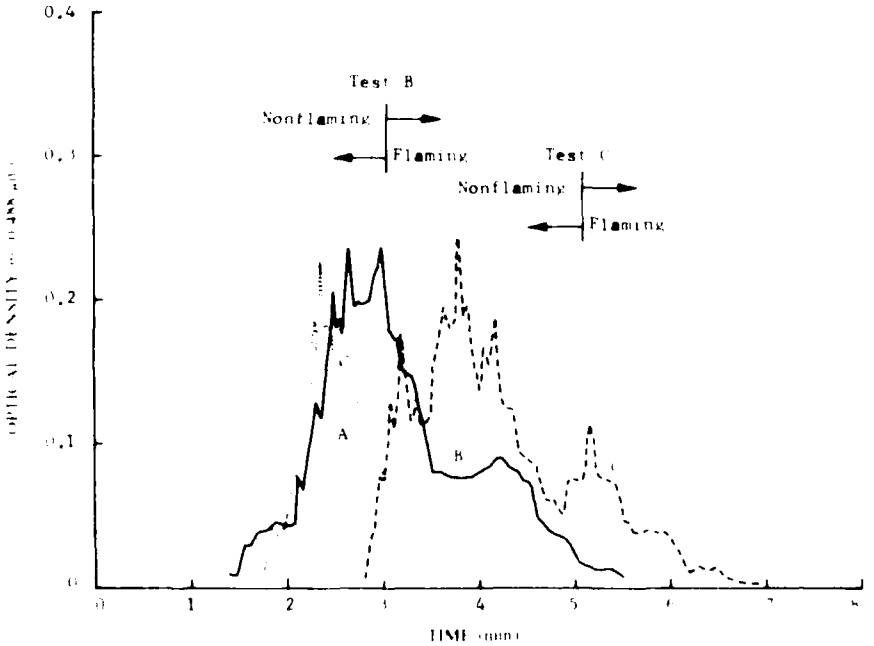

Fig. 24 — Smoke optical densities for flaming combustion of intumescent paint exposed to a radiant flux of 5 W cm^{-2} with pilot flame in heated ventilation air at 100 C

Typical plots for nonflaming tests at room temperature are shown in Fig. 25, while the corresponding data at 100°C are given in Fig. 26. For the room temperature tests, Fig. 25 shows that no single theoretical curve of $I_{\parallel}/I_{\perp}$ vs D_{32} fits the plotted points that vary steeply over a narrow range in D_{32}. This indicates that the complex refractive index varies considerably during the test, particularly near the time of peak optical density. The curve corresponding to $m_B = 1.306 - 0.0114i$ best fits the average of the $I_{\parallel}/I_{\perp}$ and OD_R/OD_B data near peak optical density (solid circles) and some of the data obtained earlier in the test. The curve corresponding to $m_B = 1.353 - 0.07i$ best fits the data obtained during the early phases of the tests; it indicates that significant variations in the complex refractive index and hence the chemical composition of the smoke particles occur during the test. This variation appears to be greatest near peak optical density where the variation of D_{32} is small.

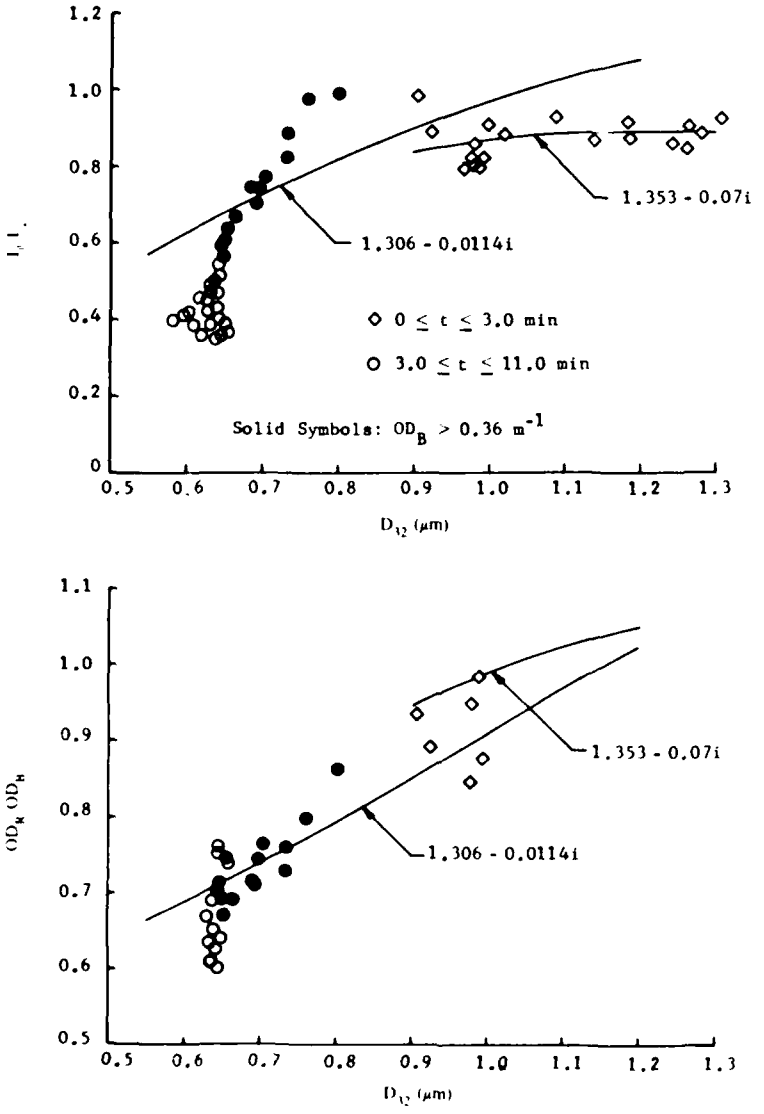

Fig. 25 Optical density ratios and 90° scattering ratios for nonflaming combustion of intumescent paint exposed to a radiant flux of 5 W/cm² in room temperature ventilation air (25°C).

Figure 26 shows the same plots for a test conducted in air heated to 100°C. Here the theoretical curve fits the plotted data near maximum optical density much more closely than in the room temperature tests. For this test the best fit of the $I/I_{\perp}$ data occurs for $n = 1.357$ and $k = 0$, indicating nonabsorbing particles. A very good fit of the OD_R/OD_B data was then obtained by allowing the refractive index to vary with wavelength ($m_B = 1.357$, $n_R = 1.346$). However, two other replicate tests yielded somewhat different results indicating absorbing particles with a somewhat smaller refractive index (about 1.33) and an absorption index of about 0.03. For these latter tests there is also considerably more deviation of the plotted points from the fitted theoretical curves than in the case illustrated by Fig. 26. The complex refractive index given in Table 8 for the nonflaming tests at 100°C is an average of values obtained from the three replicate tests discussed above.

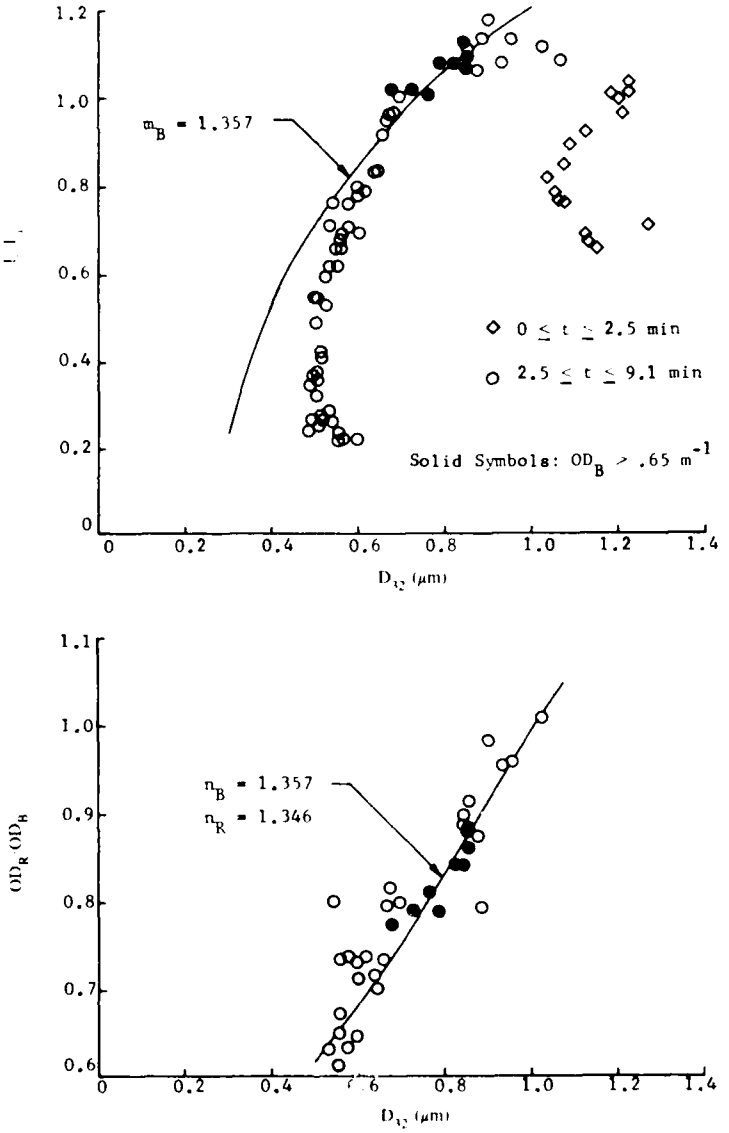

Fig. 26 — Optical density ratios and 90° scattering ratios for nonflaming combustion of intumescent paint exposed to a radiant flux of 5 W/cm² in ventilation air at 100°C

Values of the complex refractive index for nonflaming tests of the Ocean 9788 intumescent paint conducted at 150° and 200°C were obtained by a similar curve fitting process, but the data are less reliable owing to the reduction in light scattering and absorption signals at the higher temperatures. Average values of the complex refractive index shown in Table 8 suggest that for the temperature range 25° to 200°C, the absorption index k of the smoke increases steadily with ventilation air temperature and that the effect of temperature on the smoke refractive index n is small. This indicates that the chemical composition of the smoke produced during nonflaming combustion of the Ocean 9788 intumescent paint is dependent on the ventilation air temperature.

Table 8 — Smoke Refractive Index, Volume Fraction, and Total Volume for Intumescent Paint

Mode	Ventilation Air Temperature (°C)	Radiant Flux (W/cm^2)	Refractive Index m_B (NF) or m_S (F)	η_v (F)	Peak Volume Fraction (ppm)	Specific Total Particle Volume (cm^3/g)	Γ/Γ_{25}
Nonflaming	25	5.0	1.310-.010i	—	0.23	0.081	1.00
Nonflaming	100	5.0	1.341-.022i	—	0.29	0.31	0.33
Nonflaming	150	5.0	1.317-0.04i	—	0.16	0.024	0.25
Nonflaming	200	5.0	1.32-0.05i	—	0.06	0.005	0.06
Nonflaming[a]	25	5.0	1.27-0.013i	—	0.20	0.054	—
Nonflaming[a]	100	5.0	1.375-0.17i	—	0.13	0.0095	—
Flaming	100	5.0	1.206-0.15i	0.35	0.18	0.013	—
Flaming	300	5.0	1.155-0.11i	0.26	[b]	[b]	—

[a] Pilot flame on, but nonflaming combustion. At 25°C flaming never occurred, at 100°C samples ignited later in test

[b] Insufficient light attenuation for determination of volume fraction and STPV.

Figure 27 shows the particulate volume fractions for the nonflaming tests of the Ocean 9788 intumescent paint samples. These volume fractions were calculated by using the constant values of the complex refractive index given in Table 8 that were determined by the curve fitting procedure discussed above. These values of volume fraction are most reliable near the peaks where the values of complex refractive index, mean particle diameter D_{32}, and optical density used in the calculations are the most accurate. Table 8 also gives the peak volume fractions, averaged for each set of replicate tests. These peak values, which reach a maximum of about 0.3 ppm at 100°C, are considerably smaller than those obtained for the chlorinated alkyd paint under nonflaming conditions (25° and 100°C only) when the lower ventilation air flow rate of the intumescent paint tests is taken into account. The shapes of the curves of volume fraction vs time and their dependence on ventilation air temperature are similar to those of the optical density curves given in Fig. 22. This shows that the optical density of the smoke produced by the intumescent paint samples under nonflaming conditions is determined principally by its concentration.

For the case of *flaming* combustion of the Ocean 9788 intumescent paint, the soot particles produced are nonspherical and highly absorbing, and thus direct determination of the complex refractive index from the measured values of $I_\parallel/I_\perp$ and OD_R/OD_B is impossible. As in the case of the chlorinated alkyd paint, the method of downward scaling of the soot particle refractive index to account for the presence of loosely packed, low-density soot agglomerates was used. Data for the best of the flaming tests conducted in air at 100°C are shown in Fig. 28, where values of $I_\parallel/I_\perp$ are plotted vs D_{32}. This figure shows both data for the initial nonflaming phase, which lasted about 5 min., and the

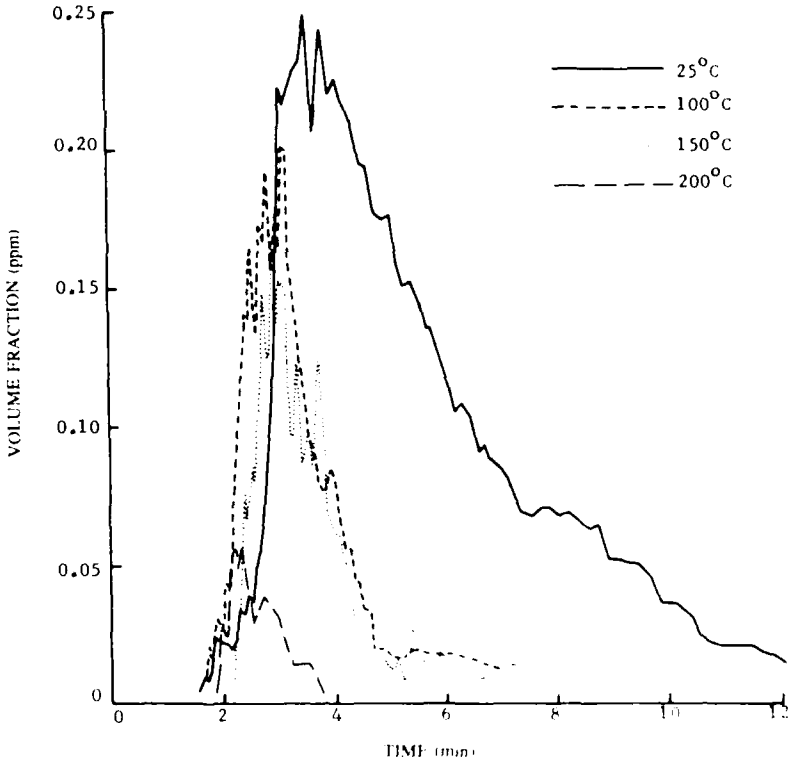

Fig. 27 — Effect of ventilation air temperature on the particulate volume fraction for nonflaming combustion of intumescent paint exposed to a radiant flux of 5 W/cm^2

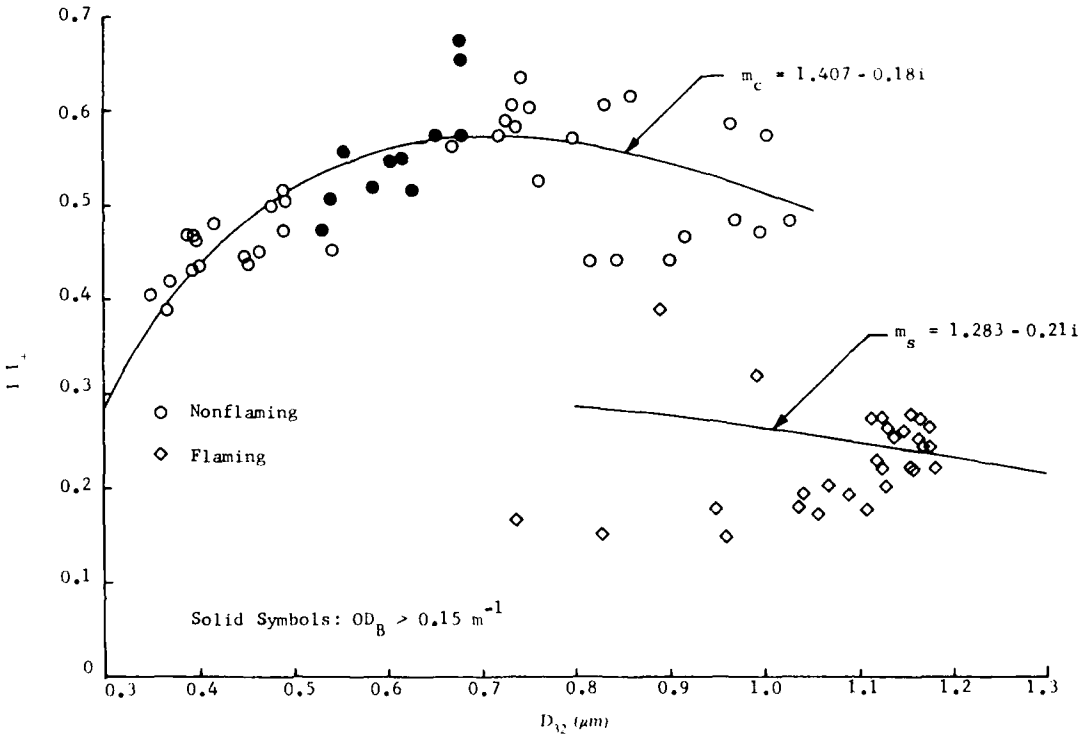

Fig. 28 — 90° scattering ratios for combustion of intumescent paint exposed to a radiant flux of 5 W/cm^2 with pilot flame in heated ventilation air at 100°C

flaming phase, which lasted about 2 min. The flaming data best fitted by an effective refractive index m_s of 1.283 − 0.21i, while the nonflaming data yielded m_B = 1.407 − 0.18i. In both cases there is considerable scatter about the theoretical curves.

Table 8 gives the averaged values of complex refractive index for both flaming m_S and nonflaming m_B phases at 100°C and flaming phases at 300°C. The corresponding values of η_v, the fraction of the optical mean particle volume that is actually occupied by the particulate material, is also given in Table 8 for the flaming phase of the tests. The η_v values indicate that the soot particulates produced during flaming combustion of the Ocean 9788 intumescent paint are very loose, low density aggregates of smaller primary soot particles similar in density to those produced by flaming combustion of the chlorinated alkyd paint. These data also indicate that the soot agglomerates produced in 100°C air are somewhat denser and more compact than those produced at 300°C.

It shoulu also be noted from Table 8 that the complex refractive index of the smoke particles produced during the nonflaming phase of the "flaming" test at 100°C (with pilot flame) was significantly different from that obtained in the purely nonflaming tests (no pilot flame). Since the absorption coefficient (imaginary part) is considerably higher when the pilot flame is lit, this difference may be due to a small quantity of soot generated by the propane flame and mixed with the smoke generated by the paint sample during the nonflaming phase of the test.

Figure 29 presents the curves showing volume fraction variations during tests of the intumescent paint with the pilot flame lit. For the test conducted in room temperature air (25°C), flaming ignition did not occur, and the resulting volume fraction curve resembles the one shown in Fig. 27 for a room temperature test without the pilot flame (i.e., radiant heating only). For Test B at 100°C, the first half of the curve (including the rising part of the sharp peak) which corresponds to nonflaming combustion, is very similar to the 100°C curve (without pilot flame) shown in Fig. 27. The onset of intermittent, localized flaming combustion produces a sudden drop in particulate volume fraction followed by a second lower peak in volume fraction for which the corresponding optical density peak shown in Fig. 24 is much less prominent. For Test C at 100°C, the second peak, which corresponds to flaming combustion, is sharper and higher than the first (nonflaming) peak. Again the corresponding optical density peak for flaming combustion (Fig. 24) is much less prominent. These differences in relative peak heights between the corresponding optical density and volume fraction curves for the 100°C tests of the Ocean 9788 intumescent paint are due to the drastic differences in mean particle diameter (Fig. 23) and complex refractive index (Fig. 28) between the smokes produced by flaming and nonflaming combustion of this material. Averaged peak volume fractions for these tests are also given in Table 8.

Values of the specific total particulate volume (STPV) are also given in Table 8. As in the case of the chlorinated alkyd paint, STPV values for *nonflaming* tests of the Ocean 9788 intumescent paint decrease markedly as the ventilation air temperature is increased. At 200°C, the STPV is only about 6% of that obtained at room temperature. For the nonflaming room temperature and 100°C tests, the STPV obtained with the intumescent paint is about twice the STPV yield of the chlorinated alkyd paint (Tables 5 and 8). In general, the total particulate volume actually produced in the intumescent paint tests was lower than that observed for the chlorinated alkyd paint owing to the much smaller sample mass used in the intumescent paint tests. Only at 100°C was it possible to measure the STPV for *flaming* combustion of the intumescent paint. The value given in Table 8 (0.013 cm^3/g) represents only the flaming portion of the test; adding the STPV value for the nonflaming part gives an STPV of about 0.023 cm^3/g for the total test, which is considerably lower than that obtained in the completely nonflaming tests.

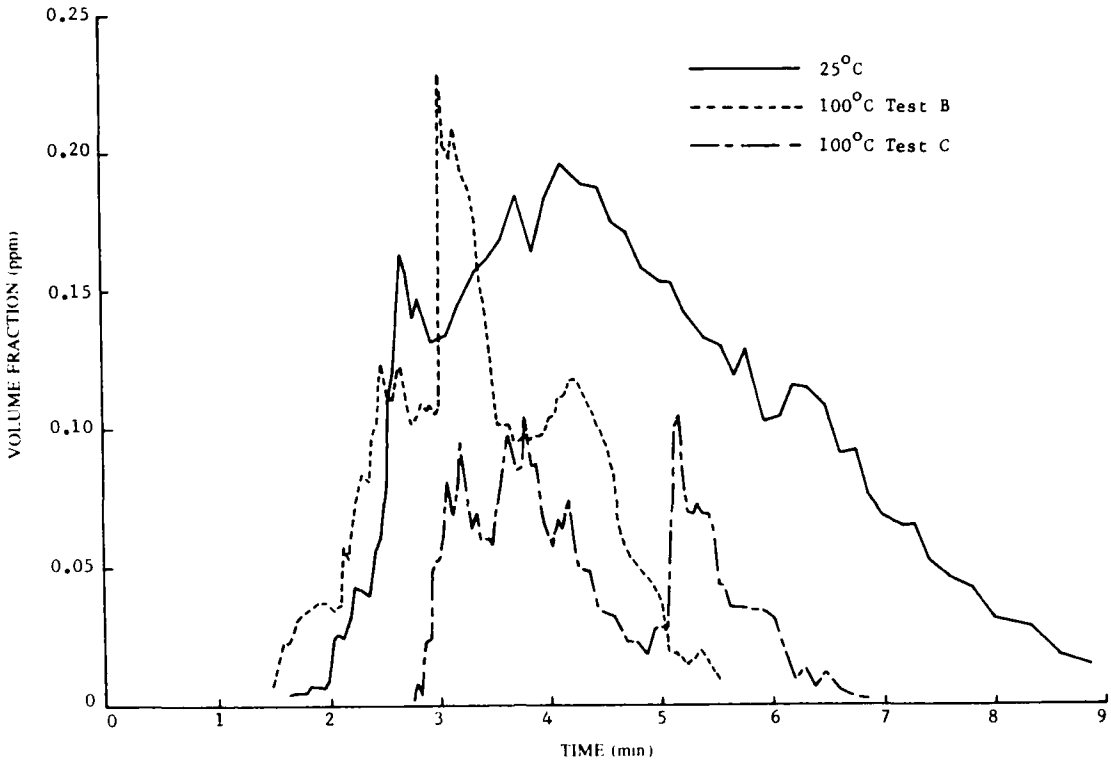

Fig. 29 — Effect of ventilation air temperature on the particulate volume fraction for combustion of intumescent paint exposed to a radiant flux of 5 W/cm^2 with pilot flame

Although no sampling data were available for elevated air temperatures, the effect on ambient temperature of Γ was estimated from the optical data. These relative values of Γ, in which Γ is normalized with respect to the corresponding room temperature value, are presented in Table 8 for nonflaming combustion only. These Γ values follow the same trend with increasing ventilation air temperature as the specific total particulate volume. Normalized Γ data were not available for flaming combustion of the intumescent paint because the 5 W/cm^2 radiant flux with pilot flame was not sufficient to ignite this material in the room temperature environment.

The total particulate masses produced in the nonflaming tests of the intumescent paint were estimated from the STPV values and the original sample masses assuming a density ρ_p = 1.3 g/cm^3 of the smoke particle material. For the room temperature tests, the optically determined values of the total particulate mass were then compared with the corresponding values estimated by particulate sampling. The sampling data was an average of the particulate masses collected for a test with cascade impactor and absolute filter in series and a test with absolute filter only. This comparison was done for tests conducted without the pilot flame and for tests conducted with the pilot flame. For nonflaming combustion without the pilot flame, the optically determined particulate mass was about 2.4 times as large as the particulate mass estimated by sampling. For nonflaming tests with the pilot flame, this ratio was about 2.0. These discrepancies are similar to those obtained for nonflaming tests of the chlorinated alkyd paint and other previously tested materials. The sources of this discrepancy are probably the same as noted for the chlorinated alkyd paint. Since particulate sampling data is not available for the tests conducted in heated ventilation air and flaming combustion did not occur in the room temperature tests, the comparison of optically determined and sampled particulate masses could not be done for flaming combustion.

By using the same procedure as described for the chlorinated alkyd paint, the values of the STPV given in Table 8 can be used to estimate the smoke volume concentration and optical density for a known quantity of Ocean 9788 intumescent paint burning in a confined space. Consider a 3.04 × 9.7 m (10 ft × 32 ft) surface (2.97 m^2) covered with three coats of intumescent paint (approximately 0.63 kg/m^2) burning in a 708-m^3 (25,000-ft^3) space. The weight of the unburned paint in this case is 18.7 kg, which is nearly the same as for the chlorinated alkyd paint example. From Table 8, the worst nonflaming case occurs for a 5.0 W/cm^2 radiant flux in room temperature air, for which the STPV is about 0.081 cm^3/g. This yields a total particulate volume of 1515 cm^3 and a volume fraction of 2.14 ppm. The resulting optical density in blue light ($\lambda = 0.488\ \mu m$) is nearly 5.4 m^{-1}, which indicates very severe attenuation of light, amounting to only 4 millionths of the incident light transmitted over a 1-m optical path length. This light obscuration is much greater than that produced by burning an equal mass of the chlorinated alkyd paint under the same conditions. A similar calculation could not be performed for flaming combustion of the intumescent paint because of the localized and intermittent nature of the flaming combustion of this paint in the small scale tests. Large scale tests of this paint applied to PVC-nitrile rubber substrates, however, shows that flaming combustion of this material does occur with the production of large quantities of black smoke [13].

SUMMARY AND CONCLUSIONS

Smoke physical properties were determined for two paints used aboard ships and submarines: a chlorinated alkyd paint as specified by DOD-E-24607 and an intumescent paint (Ocean 9788). These properties were determined for both smoldering and flaming combustion under a radiant flux of 5 W/cm^2 in both room temperature and high temperature atmospheres. The results of these tests are summarized below for each material.

Chlorinated Alkyd Paint

(a) Particle sampling indicates that the size distribution is log-normal for both nonflaming and flaming combustion of the chlorinated alkyd paint in room temperature ventilation air. For *nonflaming* combustion the smoke particulates consist of pale yellow spherical liquid droplets with a D_{MMD} of about 0.9 μm. For *flaming* combustion, black, sooty particles are produced with a D_{MMD} of about 0.6 μm. The size distribution obtained under flaming combustion is considerably broader than that produced under nonflaming combustion.

(b) During *smoldering* combustion in room temperature air, the chlorinated alkyd paint converts about 11% of its total mass loss into smoke particulates. During *flaming* combustion this material yields slightly less than 4% of its total mass loss as particulates. For both types of combustion, about 80% of the original sample mass remains after combustion as carbonaceous char and inorganic pigments.

(c) The in situ optical measurements reveal considerable variation in mean particle diameter (D_{32}) during *nonflaming* tests of the chlorinated alkyd paint in room temperature ventilation air. The D_{32} range between 0.7 and 1.1 μm, with an average of about 0.85 μm during the time of peak optical density. This latter value agrees well with the D_{MMD} obtained by sampling. For *flaming* combustion the D_{32} is nearly constant at 1.1 to 1.2 μm which is nearly twice the value obtained by sampling. This discrepancy is probably due to the nonspherical shape of these particles.

(d) The peak optical density obtained in room temperature tests at a ventilation air flow rate of 425 l/min is about 1.0 per meter for nonflaming combustion, and it is somewhat lower for flaming combustion.

(e) Smoke particles produced during *nonflaming* combustion of the chlorinated alkyd paint in room temperature air attenuate a light beam primarily by scattering, with very little, if any, absorption. These particles have a refractive index of about 1.34 during the period of maximum light obscuration. On the other hand, the smoke particles produced during *flaming* combustion of this paint are highly absorbing, with a complex refractive index consistent with loosely packed, low density soot agglomerates that occupy slightly more than 25% of the optical mean volume as determined from the forward scattering measurements.

(f) Moderate increases in the temperature of the ventilation air (to about 100°C) for *nonflaming* tests of the chlorinated alkyd paint reduce the peak optical density, peak particulate volume fraction, and specific total particulate volume (STPV) to about half of the room temperature values. Similar increases in the ventilation air temperature have little effect on D_{32} at peak optical density, but changes in the chemical composition of the particles result in light absorbing particles with a complex refractive index of approximately $1.42 - 0.1i$. Larger increases in ventilation air temperature (above 200°C) result in spontaneous ignition of the material and subsequent flaming combustion.

(g) For *flaming* combustion of the chlorinated alkyd paint there is a small but definite trend of increasing D_{32} as the ventilation air temperature is increased from 25° to 300°C. Peak values of optical density and volume fraction increase with ambient temperature, but temperature has little effect on the STPV or the complex refractive index of the smoke particles. Increased ambient temperature also slightly reduces the percentage of original sample mass remaining as char residue.

Ocean 9788 Intumescent Paint

(a) Because of the fire retardant nature of the intumescent paint, flaming combustion does not occur in room temperature air at the radiant flux of 5 W/cm^2. For tests in heated ventilation air with the pilot flame, a brief period of localized, intermittent flaming combustion is usually observed.

(b) Cascade impactor sampling indicates that the particle size distribution is log-normal for nonflaming combustion of the intumescent paint in room temperature ventilation air. The D_{MMD} average about 0.6 μm for tests conducted without the pilot flame. Microscopic examination of collected samples reveal that these particles consist of a mixture of white and light tan or beige *solid* materials.

(c) Sampling data also indicates that between 9% and 11% of the total mass loss appears as particulates during nonflaming combustion of the intumescent paint in room temperature air. Between 55% and 58% of the original sample mass remains after combustion as a thick, porous, low density carbonaceous char with a coarsely nodular surface texture.

(d) For nonflaming tests of the intumescent paint in room temperature air the mean smoke particle diameter D_{32} varies between about 1.2 μm shortly after the beginning of the test to relatively constant values of about 0.7 μm for most of the test. The optical density reaches its peak of about 0.6 per meter (142 l/min ventilation rate) just as D_{32} is leveling off to its nearly constant value. The complex refractive index of the smoke particles varies considerably during the tests, especially near the time of maximum optical density. These particles are mildly absorbing with a complex refractive index of about $1.31 - 0.01i$.

(e) The principal effect of increasing ventilation air temperature for *nonflaming* combustion of the intumescent paint is a dramatic reduction in peak optical density, peak particulate volume fraction, duration of measurable light obscuration, and specific total particulate volume for temperatures above 100°C. For ventilation temperatures of 300°C and above, light scattering and attenuation by smoke particles is negligible. The effect of environmental temperature on mean particle diameter is not

well-defined, with D_{32} ranging between 0.5 and 0.8 μm. Increasing the ventilation air temperature also increases the light absorption index of the smoke particles, which indicates an effect on chemical composition of the particles. Increasing temperature also results in a small decrease in the percentage of initial sample mass remaining as char.

(f) Smoke particles produced during the brief periods of intermittent, localized flaming combustion in the 100° and 300°C atmospheres, appear to consist of loose agglomerates of smaller soot particles. These agglomerates have optical mean diameters ranging between 1.2 and 1.35 μm.

The smoke physical properties of the two paints tested in this program may be compared by taking into account the differences in initial sample masses and ventilation air-flow rates for these two materials. For nonflaming combustion, the smoking tendency Γ of the two paints is about the same. The intumescent paint produces somewhat smaller particles than the chlorinated alkyd paint during nonflaming combustion and slightly larger particles during flaming combustion. For nonflaming combustion, the particles produced by the two paints differ greatly in shape, chemical composition, and physical state. For flaming combustion both paints yield loosely packed, low density agglomerates of smaller primary soot particles. Most significantly, the STPV produced by the intumescent paint during nonflaming combustion in room temperature air is about twice that produced by the chlorinated alkyd paint under the same conditions. Thus, the resulting light obscuration obtained with the intumescent paint is much greater than that produced by burning an equal mass of chlorinated alkyd paint under nonflaming, room temperature conditions. This comparison could not be made for flaming combustion because of the localized and intermittent nature of the flaming combustion of the intumescent paint.

REFERENCES

1. C.P. Bankston, R.A. Cassanova, E.A. Powell, and B.T. Zinn, "Initial Data on the Physical Properties of Smoke Produced by Burning Materials Under Different Conditions," *J. Fire and Flammability* 7, 165-180 (1976).

2. C.P. Bankston, "Determination of the Physical Characteristics of Smoke Particulates Generated by Burning Polymers," Ph.D. Thesis, School of Aerospace Engineering, Georgia Institute of Technology, 1976.

3. E.A. Powell, C.P. Bankston, R.A. Cassanova, and B. T. Zinn, "The Effect of Environmental Temperature upon the Physical Characteristics of the Smoke Produced by Burning Wood and PVC Samples," *Fire and Materials* **3**(1), 15-22 (1979).

4. B.T. Zinn, R.F. Browner, E.A. Powell, M. Pasternak, and R.O. Gardner, "The Smoke Hazards Resulting from the Burning of Shipboard Materials Used by the U.S. Navy," NRL Report 8414, July 1980.

5. F.W. Williams, B.T. Zinn, R.F. Browner, and E.A. Powell, "The Smoke Hazards Resulting from the Burning of Shipboard Materials Used by the U.S. Navy - Part II," NRL Report 8990, October 1986.

6. E.A. Powell, R.A. Cassanova, C.P. Bankston, and B.T. Zinn, "Combustion-Generated Smoke Diagnostics by Means of Optical Measurement Techniques," in Experimental Diagnostics in Gas Phase Combustion Systems *(Progress in Astronautics and Aeronautics*, Vol. 53), Ben T. Zinn, ed. (American Institute of Aeronautics and Astronautics, New York, 1977), p. 449.

7. E.A. Powell and B.T. Zinn, "In Situ Measurements of the Complex Refractive Index of Combustion Generated Particulates," in Combustion Diagnostics by Nonintrusive Methods *(Progress in Astronautics and Aeronautics*, Vol. 92), T.D. McCay and J.A. Roux, eds. (American Institute of Aeronautics and Astronautics, New York, 1984), pp. 208-237.

8. B.T. Zinn, E.A. Powell, R.F. Browner, and M. Pasternak, "The Smoke Hazards Resulting from the Burning of Shipboard Materials Used by the U.S. Navy – Polyphosphazene Insulation," NRL Report on Contract No. N000-80-C-0432, 1984.

9. "Military Specification: Enamel, Interior, Nonflaming (Dry), Chlorinated Alkyd Resin, Semigloss," DoD-E-24607, Amendment 1, 16 December 1981.

10. I. Glassman, "Phenomenological Models of Soot Processes in Combustion Systems," AFOSR TR-79-1147.

11. R.A. Dobbins, R.J. Santoro, and H.G. Semerjian, "Interpretation of Optical Measurements of Soot in Flames," in Combustion Diagnostics by Nonintrusive Methods *(Progress in Astronautics and Aeronautics*, Vol. 92), T.D. McCay and J.A. Roux, eds. (American Institute of Aeronautics and Astronautics, New York, 1984), pp. 208-237.

12. S.C. Graham, "The Refractive Indices of Isolated and Aggregated Soot Particles," *Combustion Science and Technology*, **9**, pp. 159-163 (1974).

13. J.I. Alexander, D.J. Bogan, S.L. Brandow, H.W. Carhart, H.G. Eaton, C.R. Kaplan, S.R. Lustig, R.M. Neilon, E.A. Powell, H.J. St. Aubin, R.S. Sheinson, M.B. Simmons, J.S. Stone, T.T. Street, P.A. Tatem, M.R. Wagner, T.M. White, and F.W. Williams, "Submarine Hull Insulation Fires—Suppression with Nitrogen Pressurization and Corrosion Rates of Metals," NRL Report 8943, Feb. 1986.

END

12-87

DTIC